ISSN 2595-2137 / e-ISSN 2674-8568

Volume 2 • Number 4 • December 2019

JOURNAL OF BIOENGINEERING AND TECHNOLOGY APPLIED TO HEALTH

An Official Publication of the Health Institute of Technology - ITS/SENAI CIMATEC

PUBLISHED BY SENAI CIMATEC

December 2019
Printed in Brazil

JOURNAL OF BIOENGINEERING AND TECHNOLOGY APPLIED TO HEALTH

An Official Publication of the Health Institute of Technology - ITS/SENAI CIMATEC

JOURNAL OF BIOENGINEERING AND TECHNOLOGY APPLIED TO HEALTH

Volume 2 • Number 4 *December 2019*

The Journal of Bioengineering and Technology Applied to Health (JBTH) is an official publication of the Health Institute of Technology – ITS /SENAI CIMATEC. It is published quarterly (March - June - September - December) in English by SENAI CIMATEC – Avenida Orlando Gomes, 1845, Piatã, Zip Code: 41650-010, Salvador-Bahia-Brazil; phone: (55 71) 3879-5501. The editorial offices are at Health Institute of Technology at SENAI CIMATEC.

Editorial Office

Correspondence concerning subscriptions, advertisements, claims for missing issues, changes of address, and communications to the editors should be addressed to the Deputy Editor, Dr. Roberto Badaró, Journal of Bioengineering and Technology Applied to Health – JBTH – Avenida Orlando Gomes, 1845, Piatã, Zip code: 41650-010, Salvador-Bahia-Brazil; phone: (55 71) 3879-5501; or sent by e-mail: jbth@jbth.com.br

Permissions

Postmaster

Send address changes to JBTH, Avenida Orlando Gomes, 1845, Piatã, Zip Code: 41650-010, Salvador-Bahia-Brazil.

Information by JBTH-ITS/SENAI CIMATEC

Home-page: www.jbth.com.br
E-mail: jbth@jbth.com.br
Phone: (55 71) 3879-5501 / 3462-9599
ISSN: 2595-2137
e-ISSN 2674-8568

https:// jbth.v2i4

Copyright

COVER: Morphological characteristics of HEPA-1c1c7 tumor cells exposed to jararhagin for 24 hours at different concentrations. Article: Effect of Snake Venom Metalloprotease Desintegrin in Hepatocarcinoma Tumor Cells. Durvanei Augusto Maria et al. 2019;2(4):119.All rights reserved.

Contributions and Impacts on Health Using New Technologies and Innovative Products

Lílian Lefol Nani Guarieiro[1]*; Alex Álisson Bandeira Santos[2]
[1,2]Centro Universitário Senai Cimatec, Integrated Campus of Manufacturing and Technology; Salvador, Bahia, Brazil

This edition of the **Journal of Bioengineering and Technology Applied to Health** brings a selection of four articles presented at the V International Symposium on Innovation and Technology (SIINTEC).

The SIINTEC happens since 2015 at SENAI CIMATEC. The event is annual and promoted by SENAI CIMATEC, Salvador, Bahia, Brazil. The objective of the event is to contribute significantly to the scientific and technological country's development, seeking the massive participation of academy and industry involved in research, development and innovation.

The V SIINTEC was held from October 9th to October 11th, 2019, and had focus on: "Circular Economy".

The event gave the opportunity to discuss the main topics related to technological innovations as basis for meeting the challenges of productive processes for the generation and application of business and social.

The contributions and impacts on health using new technologies and innovative products are discussed in the papers selected for publication.

The topics discussed bring discussions about:

- Humanoid prototype development through 3D printing for new technologies;
- Mathematical modeling of the extraction process essential oils;
- The Impact on Human Health of Particulate Matter Arising from Atmospheric Pollution;
- An Innovative Concept of Traceable Device for Monitoring Temperature of Healthcare Products Temperature Sensitive.

The research presented in this edition makes significant contributions to state-of-the-art presentations, innovative medical products, health innovation initiatives, and a review article.

The authors highlighted in their research:

1. The development of a prototype of a humanoid robot by 3D printing that is as close as possible to the human being;
2. Supercritical oil extraction from *S. terebinthifolius* can result in higher value-added products when integrated to Mathematical models;
3. The fine particles (PM2.5) are the most recurrent incidence of respiratory disease, as they are emitted mainly by industrial activities and vehicular emissions; and
4. The thermo-sensitive health products lack traceability in the health network and that the concept presented contributes to preserving their integrity along the cold chain.

We wish you all an excellent reading.

Received on 27 September 2019; revised 13 October 2019.Address for correspondence: Dr. Lílian Lefol Nani Guarieiro. Centro Universitário SENAI CIMATEC. Av. Orlando Gomes, 1845, Piatã. Zip Code: 41650-010. Salvador, Bahia, Brazil. E-mail: lilian.guarieiro@fieb.org.br. DOI: https://doi.org/10.34178/jbth.v2i4.88
J Bioeng. Biotech. Appl. Health 2019;2(4):111.

Effect of Snake Venom Metalloprotease Desintegrin in Hepatocarcinoma Tumor Cells

Amanda Gomes[1]; Leticia Monica Coimbra Gaziola[2]; Luciana Knop[3]; Rosa Andrea Nogueira Laiso[2]; Durvanei Augusto Maria[1,2]*

[1]Medicine School of University of São Paulo; [2]Laboratory of Molecular Biology, Butantan Insitutite; São Paulo, São Paulo;[3]Health Institute of Technologies – SENAI-CIMATEC; Salvador, Bahia; Brazil

Hepatocellular carcinoma is the third leading cause of cancer-related death in the world. This cancer is associated with cirrhosis following the hepatitis B or C virus infection, alcohol addiction, metabolic liver disease and exposure to dietary toxins such as aflatoxins and aristolochic acid. Studies demonstrate the integration of the HBV genome into liver cell DNA, including cases of patients with HBV-negative serology. Despite advances in prevention techniques, screening, and technology in cancer diagnosis and treatments, the incidence and mortality remain worrisome. Therefore, this research is significant due to the contribution of the development of new biological agents that can be used as monotherapy or adjuvant chemotherapy. Jararhagin, a snake toxin isolated from *Bothrops jararaca* venom, has been the subject of many studies seeking alternatives for the treatment of cancer. This protein contains the cysteine-rich disintegrin-like metalloproteinase domains and desirable functions to combat tumor cells, such as promoting acute inflammation, damaging the vascular endothelium through the zinc-dependent catalytic domain (responsible for hemorrhagic function) and enzymatically degrading the constituents of the endothelial basement membrane. Due to the antitumor effects of jararhagin presented in previous research, this study aimed to describe the possible antitumor effects of this snake metalloprotease in the murine liver tumor, intending to propose a new therapeutic option in the human liver tumor.
Keywords: Cancer. HCC. Hepatocellular. Jararhagin. Metalloprotease.

Among the primary liver tumors, the most common is hepatocellular carcinoma (HCC), an aggressive disease that occurs in more than 80% of liver cancer cases [1]. HCC is the third leading cause of cancer-related death in the world. Although there are advances related to prevention techniques, screening, technology in diagnosis and treatment of cancer, the incidence and mortality remain worrisome [2,3]. In western countries, including Brazil, 70%-80% of HCC cases are associated with cirrhosis following chronic hepatitis B (HBV) or C (HCV) infection. This cancer is significantly linked to cases of HBV infection due to genome integration from the virus to the hepatocyte's DNA. Still, there are patients with hepatitis B virus-negative serology and HBV in their tumor. Alcohol is also a factor associated with predisposition to liver cirrhosis and, consequently, to HCC, as 80%-90% of patients with HCC have cirrhosis regardless of this etiology [4]. In the United States, alcohol consumption is a relevant risk factor, since the country reports alcohol abuse as a cause related to the development of the disease five times more than hepatitis C [3,5].

In the treatment of HCC in advanced stages, the indication of sorafenib, a tyrosine kinase inhibitor, is well advised. However, its use as an adjuvant after partial hepatectomy for HCC is not yet well-established. A randomized clinical trial comparing sorafenib to placebo involving 1,114 patients on adjunctive therapy after partial hepatectomy or HCC ablation was recently completed. In this study, 900 patients received surgical treatment for HCC. However, this trial demonstrated that there is no statistical difference in survival between the group of patients receiving sorafenib and the control group [5].

Liver cancer survival rate is up to 5 years after diagnosis [6], following the same relative 5-year survival for all cancers. Data reveal that cancer

Received on 24 September 2019; revised 11 October 2019.
Address for correspondence: Prof. Dr.Durvanei Augusto Maria. Institute of Butantan, Biology Molecular Laboratory, Avenida Vital Brasil, Number 1500, Zip Code: 05503-900, São Paulo, SP, Brazil. Phone/Fax: (5511)2627-9750. E-mail: durvanei@usp.br. DOI: https://doi.org/10.34178/jbth.v2i4.89

J Bioeng. Biotech. Appl. Health 2019;2(4):112-122.

survival has increased significantly over the past three decades, in part due to targeted therapy. Nevertheless, there are still many site-specific medications that may play a role only in a portion of cancer patients who have specific molecular changes. It is necessary to continue developing new biological agents that can be used alone and/or as adjuvant therapy in protocols with current chemotherapic drugs already approved by the competent organs [7].

In this context, jararhagin (snake toxin isolated from *Bothrops jararaca* venom) has been the subject of many studies seeking alternatives for the treatment of cancer. This protein contains the cysteine-rich disintegrin-like metalloproteinase domains and desirable functions to combat tumor cells, such as promoting acute inflammation, damaging the vascular endothelium through the zinc-dependent catalytic domain (responsible for hemorrhagic function) and enzymatically degrading the constituents of the endothelial basement membrane [8,9].

A study of jararhagin-treated cell culture macrophages showed increased expression of proinflammatory mediators, including IL-1, a cytokine that induces inflammation associated with expression of adhesion molecules such as CD44 invasion and migration marker, CD34 angiogenesis marker, increased TNF-alpha, crucial in the development of jararhagin-induced necrosis, and the release of chemotaxis mediators [10].

In other study, low-dose jararhagin-induced effects were antiproliferation and induction of cell death of SK-Mel-28 lineage melanoma cells, which was also supported by increased expression of cell cycle-related genes and apoptosis [9]. Jararhagin also showed cytotoxicity in breast tumor cells. Promoting alterations in the cell cycle, death of tumor cells by necrosis, even due to high inflammatory intensity, reduced viability of tumor cells [10].

Due to the antitumor effects of jararhagin presented in previous research, this study aimed to elucidate the possible antitumor effects of this snake venom metalloprotease in the murine liver tumor, aiming to propose a new therapeutic option in the human liver tumor.

Methods

Monolayer Cell Culture

HEPA-1c1c7 murine hepatocarcinoma cell lines, code CRL-2026 originating from the American Type Culture Collection (ATCC), were used, maintained, and stored in the cell bank by Dr. Durvanei Augusto Maria (Biology Molecular Lab., Butantan Institute). After thawing, the cells were transferred to a cell culture bottle (25 cm^2) containing DMEM and MEM-α culture medium (Cultilab, Campinas-SP), respectively, supplemented with 10% fetal bovine serum, 200 mM sodium bicarbonate, pH 7.4 in an oven 5% CO_2 at 37°C. Monolayer cells were subjected to enzymatic dissociation with 0.2% trypsin solution + 0.02% EDTA to detach the cells. Enzyme neutralization was performed using the same DMEM culture medium containing 10% SFB. After neutralization, the suspended cells were counted in a Neubauer chamber, and the concentration adjusted to 10^5 cells/mL. The Trypan blue exclusion test determined cell viability.

Determination of Cytotoxic Activity by MTT Method

Tumor cells were incubated in 96-well plates at a concentration of $2x10^5$cells/mL for 24 hours and treated with jararhagin at multiple concentrations. The culture medium was used as a Control Group to dilute the jararhagin stock solution. After 24 hours of treatment, the supernatant was collected on another plate, and 100 µL of MTT (Calbiochem - Darmstadt, Germany) added at a concentration of 5 mg/mL; then the cells were incubated for 3 hours in an oven containing 5% CO_2 at 37°C.W. Afterwards, the contents werere moved and 100µL of methylalcohol was added to dissolve the formed and precipitated formazan crystals. Absorbance quantification was performed in a 540nm wavelength ELISA reader. Toxicity-inducing concentration in 50% of cells (IC50%) was determined at treatment after 24 hours at different concentrations to assess the dose-response effect. The percentage of cell death, calculated concerning the negative-control, expressed the cytotoxicity of each treatment.

Determination of Polyunsaturated Lipid Peroxidation Products

The cell culture supernatants used for the MTT cytotoxicity test and kept under refrigeration at -20°C. The samples were thawed at room temperature. Then 50 µL of the sample was added in microtube, along with 250 µL of trichloroacetic acid - 20% TCA (Sigma-Aldrich) in other microtube, 50 µL of the same sample was added with 250 µL of thiobarbituric acid - TBA 0.86% (Sigma-Aldrich, Cat.: T550-0). The microtubes were placed in a water bath (100°C) for 20 minutes, followed by cooling at 0°C for 20 minutes, centrifugation at 8,000 rpm for 4 minutes, and the supernatant was used to quantify TBARS. The reading was performed on the spectrophotometer at a wavelength of 535 nm.

Morphological and Marker Analysis with Confocal Laser Microscopy

An aliquot of HEPA-1c1c7 tumor cell culture grown in a 24-well plate and coverslip with 10% SFBMEM-α culture medium kept in the oven at 5% CO_2 at 37°C. Cell samples from the Jararhagin-treated Groups and Control Group shave gone through a culture medium removal process, then 1 mL of paraformaldehyde was added to fix the cells. After this process, 1 mL of 2 times of PBS was added for washing, and also 300 µL of bovine serum albumin (BSA) for 10 minutes, then a new PBS wash was performed. After that, 10uL of Triton-X was added and incubated for 1 hour. Afterward, it was added in each well-plate over the coverslips containing the cells, 1 uL of CD44 and CD34 antibodies labeled with green fluorescein isothiocyanate (FITC) and Caspase 3, PE53 and COX-2 labeled with PE (Phycoerythrin) red fluorochrome. The plate remained overnight in the refrigerator at -4ºC. After this process, 3 washes with 1 PBS-time were performed. Then, PBS washes were performed 3 times. The coverslips were mounted, and 3 µL of the mounting medium for fluorescence protection (Fluoroshield, Sigma-Aldrich) were placed on them. The assembled blades were wrapped in aluminum foil to protect fluorescence and stored at 4°C until visualization.

Scanning Electron Microscope (SEM)

Jararhagin-treated HEPA-1c1c7 ($5x10^5$) tumor cells were washed for 24 hours with PBS and fixed in 2.5% glutaraldehyde, pH 7.2 at 4°C. After 24 hours of fixation, the cells were washed in a Na_3PO_4 buffer and were post-fixed in 1% osmium tethoxide for 2 hours at 4°C. Samples were dehydrated in increasing ethanol series, immersed in isoamylacetate and critical-point dried in liquid CO_2 for 5 minutes. The samples were atomized and coated with gold metal and examined on the Leo 435VP Zeiss Scanning Electron Microscope (Carl Zeiss,Germany).

Cell Cycle Phases Analysis by Flow Cytometry

After confluence in the 6-well plate, the cells were subjected to jararhagin treatment for 24 hours. The Control Group was from the same cell lineage, but not treated. The cells were then trypsinized and resuspended in PBS, centrifuged twice at 3,000 rpm with PBS solution and resuspended in 200 µL propidium iodide solution (18ug) (Sigma-Aldrich) containing 20 uL Triton X-100 (Sigma-Aldrich) and 4 mg RNAse-A (Molecular Probes) for 30 minutes at room temperature, protected from light. After this period, the samples were transferred to cytometry tubes, and the images were captured in a flow cytometer (Facscalibur-Becton and DicKson).

Results

Determination of Cytotoxic Activity by MTT Method

After 24 hours of adhesion, in a 96-well plate, the cells were incubated, diluted in culture medium at 10% of fetal bovine serum and 1% of penicillin antibiotic with different jararhagin concentrations of 0.001nM - 1µM.

After treatment with jararhagin, the HEPA-1c1c7 tumor cells showed morphological alterations, such as cell lysis and the formation of cell debris, from the concentration of 11.9nM (Figures 1, 2, 4, 5, 6). The other concentrations showed cytotoxic effects, with the percentage increase in cell mortality, loss of cell adhesion,

cytoplasmic membrane fragmentation, and loss of cytoplasmic prolongation progression.

Determination of Lipoperoxidation (LPO) Products by Quantification of Thiobarbituric Acid Reactive Substances (TBARS) (Figure 3)

Thiobarbituric acid reactive substances (TBARs) method quantified lipid peroxidation in cell membranes and free radical formation. Malondialdehyde (MDA) is one of the end products of lipoperoxidation formed by the primary or secondary decomposition of intermediate products, and reacts with thiobarbituric acid were widely used in the determination of oxidative stress.

Jararhagin treatment resulted in a significant formation of lipid peroxidized radicals from the hepatocarcinoma tumor lineage, with significant oxidative damage from 19.8nM concentrations. There is a positive correlation between the effects of jararhagin and the production of lipoperoxidation radicals. Quantification of TBARs revealed lower free radical production at high concentrations, which increased progressively with longer incubation time with jararhagin.

Morphological and Marker Analysis with Confocal Laser Microscopy

In this project, confocal laser microscopy was used to visualize morphological alterations of HEPA-1c1c7 tumor cells after 24 hours of jararhagin treatment at concentrations of 128.7nM and 186.2nM.

Morphological Alterations in Jararhagin-Treated HEPA-1C1C7 Tumor Cells

Jararhagin was used to elucidate the role of the disintegrin domain of this toxin on the induced effects on liver carcinoma tumor cells as an experimental model to evaluate the possible mechanisms of inhibition of proliferation and metastases. The morphological effects on HEPA-1c1c7 tumor cells were dose and time- dependent. These effects include loss of cytoplasmic expansions, round-shaped cellular aggregates, and cell detachment to the bottom of bottles and formation of apoptotic bodies, as demonstrated by scanning electron microscopy (Figure 6), similar to the cytological results obtained by Corrêa and colleagues (2002) and Klein and colleagues (2011) in human melanoma cells SK-Mel-28 [9,14].

The morphology was dramatically altered by treatment with the toxin. Scanning electron microscopy (SEM) showed that monolayer-grown hepatocarcinoma cells showed changes in an extracellular matrix organization with significant deposition and dense extracellular matrix synthesis when compared to untreated Control Group cells (A, B, C - Control Group - Figure 5) (D-I Jararhagin-treated Group - Figure 5). Tumor cells showed retraction and aggregates with jararhagin treatment at 128.7nM concentration (Figures 5 D, E, F). The 186.2nM treated tumor cells showed detachment of the plaque surface and formation of smaller aggregates, apoptotic bodies, and necrotic debris (Figure 5 G, H, I). Arrows show the formation of apoptotic bodies (12,000x).

Cell Cycle Phases Analysis by Flow Cytometry

The effect of jararhagin on cell cycle phases was determined after evaluating cell viability by MTT methods. The concentrations of 128.7nM and 186.2nM were selected. Cell aggregates were collected from both supernatant and adherent cells after trypsinization and evaluated by flow cytometry. Histograms show the percentage of cells distributed in the different phases of the G0 /G1, S, and G2/M cell cycle and sub-G1cells (Figure 7).

We observed that jararhagin changes the proportion of cells at different stages of the cell cycle. Figure 3 presented the value of the mean percentage ± sd of cells in the cell cycle phases of HEPA-1c1c7 tumor cells. The jararhagin treatment induced increased populations with fragmented DNA and G2/M arrest. The 186.6nM concentration of jararagine induced a four-times increase in the proportion of cells in the sub-G1 phase, demonstrating their potential for cytotoxicity.

Figure 1. Appearance of the cellular alterations presented after the jararhagin treatment of HEPA-1c1c7 tumor cells.

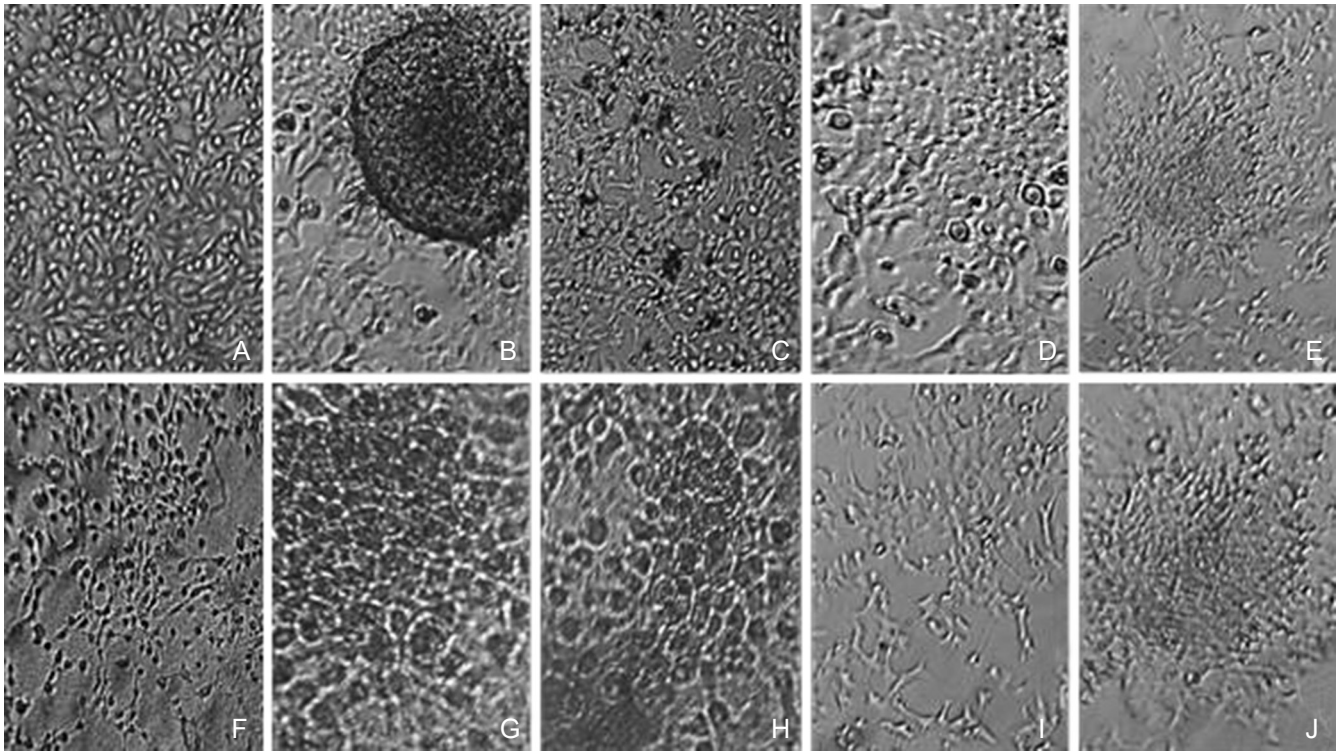

(A) Control Group. (B) Jararhagin-treated Goup with 0.001nM concentration. Significant changes were observed in morphology and cell adhesion. (C) Jararhagin-treated Goup with 0.001nM concentration presented a moderate loss of cell adhesion and morphological alterations with consequent cell death; (D) Jararhagin-treated Goup with 0.13nM concentration showed moderate loss of cell adhesion and morphological alterations. In the other concentrations, from 1.5nM to 1µM, there were slight changes in cell morphology.

Figure 2. Inhibitory concentration (50%) obtained by the equation of a line at 186.2nM.

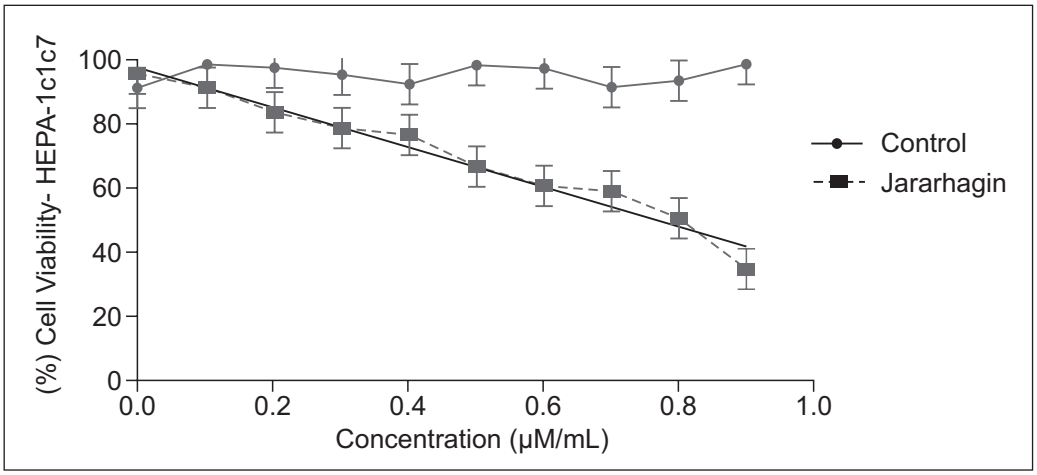

The number of experiments performed n=8. * Significant differences between the Jararhagin-treated Group and Control Group. ANOVA Variance Test followed by Tukey Kramer's Multiple Test. $p<0.001$.

Figure 3. Mean values ± standard deviation of malondialdehyde (MDA) lipopedoxidation.

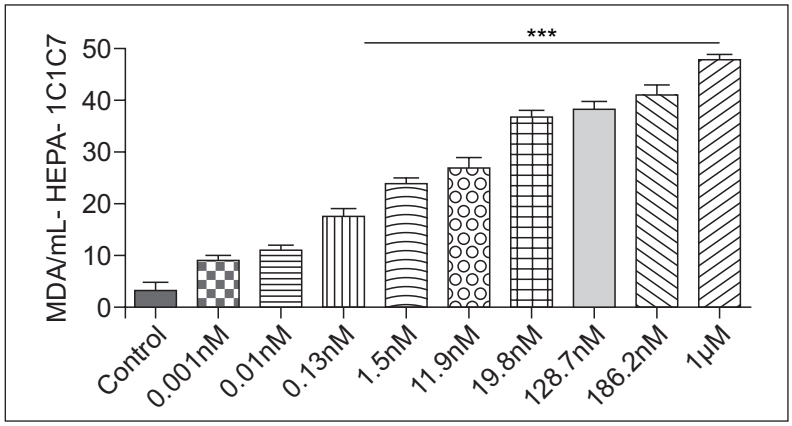

Number of experiments performed n=8. * Significant differences between the Jararhagin-treated Group and Control Group. ANOVA Variance Test followed by Tukey Kramer's Multiple Test. $p<0.001$.

Figure 4. Photomicrograph of monolayer culture of HEPA-1c1c7 tumor cells acquired by confocal laser microscopy.

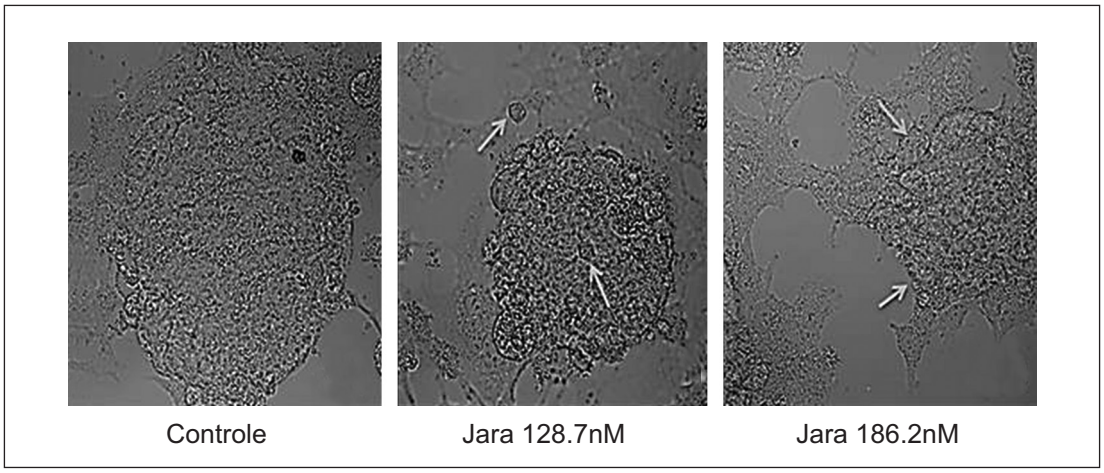

(A) Control Group - cells show epithelial morphology. (B) Jararhagin-treated Group at 128.7nM concentration - cells undergoing necrosis and apoptosis. (C) Jararhagin-treated Group at 186.2nM concentration - cells undergoing necrosis and apoptosis, with retraction of the cytoplasm and formation of apoptotic bodies. White arrows: apoptotic bodies; necrotic structures with the pyknotic nucleus.

Discussion

Several types of research involving cell cultures evaluate toxins isolated from snake venom and the effects on several tumor cell lines, aiming to find substances with possible therapeutic potential, acting as a single or adjuvant chemotherapeutic agent[11].

According to Moura and colleagues [12], jararhagin hemorrhagic activity is related to jararhagin specificity by α2β1 integrins expressed in endothelial cells [12]. One study demonstrated the pronounced expression of these integrins during embryonic development, as well as the fragility of capillaries that are constituted of a single layer of endothelial cells. The basal lamina appearing on the eighth day [13], a fact demonstrated by hemorrhage provoked by jararhagin in a time/dose-dependent form on this study.

Figure 5. Photomicrograph of monolayer culture of HEPA-1c1c7 tumor cells acquired by confocal laser microscopy.

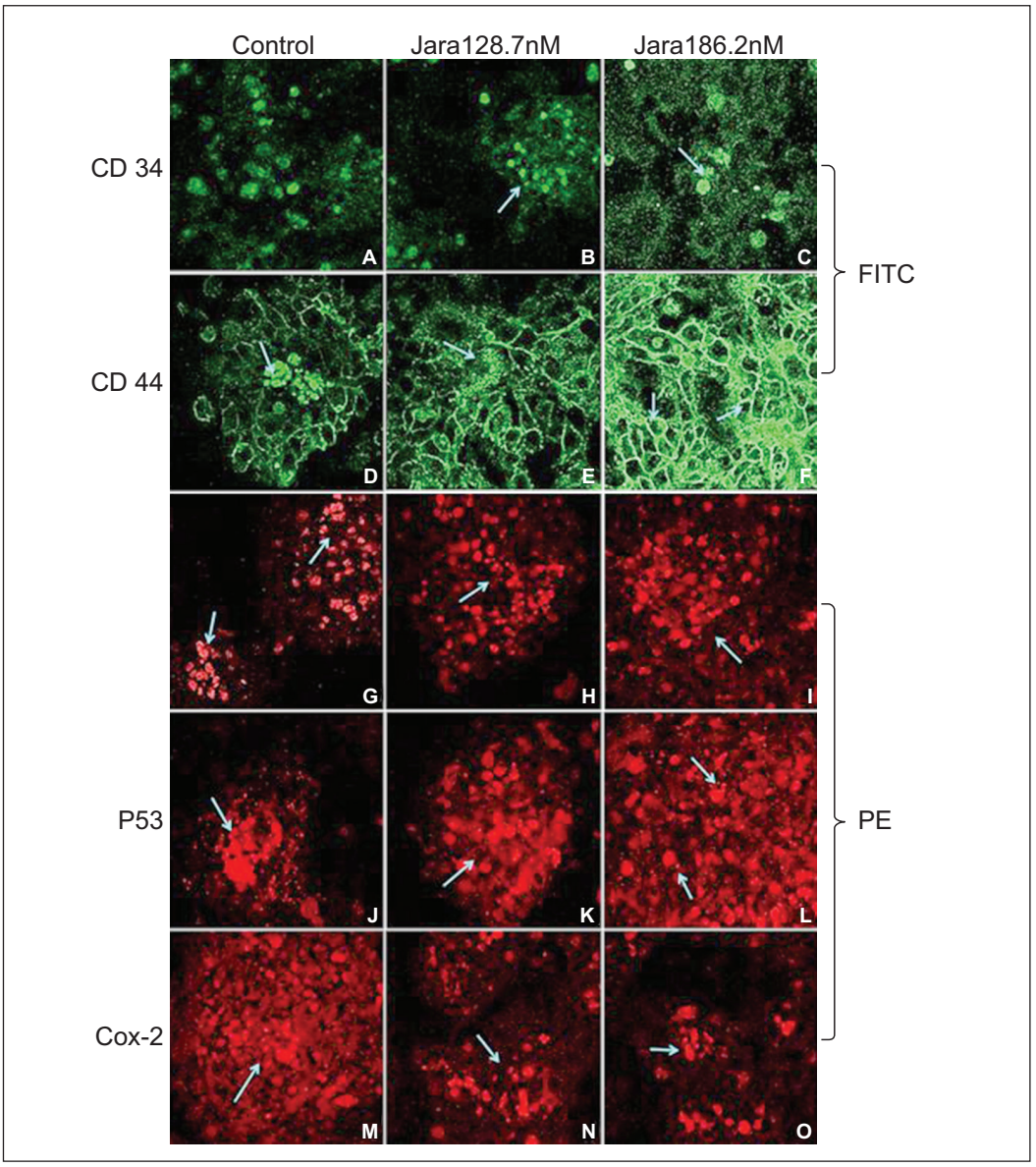

(A) CD-34 protein expression in the Control Group. (B) CD-34 protein expression in the Jararhagin-treated Group at 128.7nM concentration - cells were undergoing necrosis and apoptosis. (C) Expression of CD-34 protein in the Jararhagin-treated Group at 186.2nM concentration. (D) CD-44 protein expression in the Control Group. (E) CD-44 protein expression in the Jararhagin-treated Group at 128.7nM concentration - cells were undergoing necrosis and apoptosis. (F) CD-44 protein expression in the Jararhagin-treated Group at 186.2nM concentration. (G) Caspase-3 protein expression in the Control Group. (H) Caspase-3 protein expression in the Jararhagin-treated Group at 128.7nM concentration - cells were undergoing necrosis and apoptosis. (I) Caspase-3 protein expression in the Jararhagin-treated Group at 186.2nM concentration. (J) P53 protein expression in the Control Group. (K) P53 protein expression in the Jararhagin-treated Group at 128.7nM concentration - cells were undergoing necrosis and apoptosis. (L) P53 protein expression in the Jararhagin-treated Group at 186.2nM concentration. (M) Cox-2 protein expression in the Control Group (N) Cox-2 protein expression in the Jararhagin-treated Group at 128.7nM concentration - cells were undergoing necrosis and apoptosis. (O) Cox-2 protein expression in the Jararhagin-treated Group at 186.2nM concentration. The arrows show points where there was a pronounced expression of each protein analyzed, respectively.

Figure 6. Morphological characteristics of HEPA-1c1c7 tumor cells exposed to jararhagin for 24 hours at different concentrations.

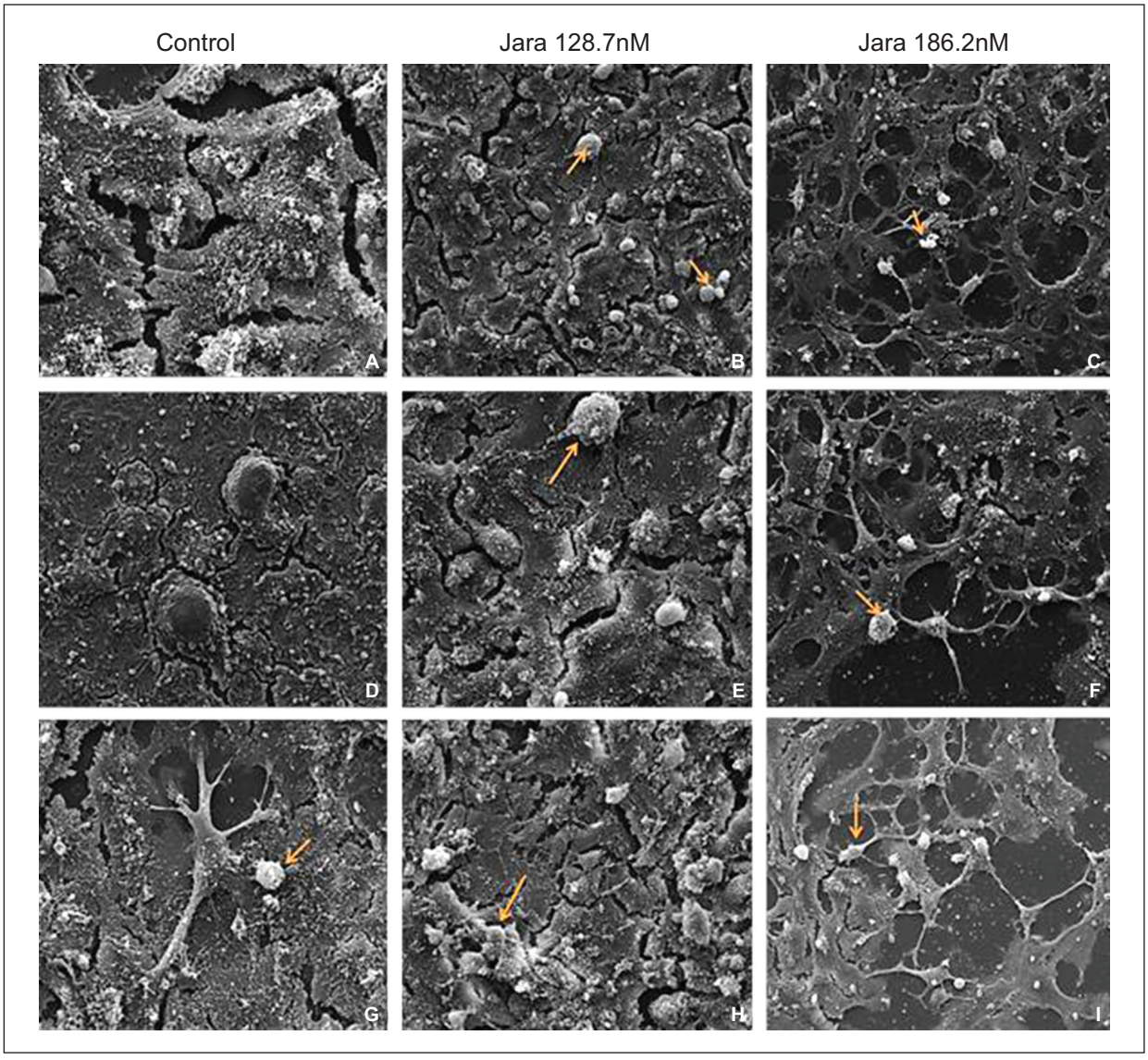

Jararhagin, isolated from *Bothrops jararaca* venom, induces changes in the morphology and viability of human melanoma cells (SK-MEL-28), in addition to reducing *in vivo* the number of metastases when pretreated and injected in mice, according to data obtained by our research group in 2011 [9]. Besides, the jararhagin treatment also promotes morphological alterations such as cytoplasmic retraction, loss of adhesion and formation of large multicellular aggregates. These changes were accompanied by decreased expression of the CDK2 and CDK4 genes, promoting an increase in the population of cells in S-phase of the cell cycle[14].

In this study, the cytotoxic effects in HEPA-1c1c7 murine hepatocellular carcinoma cells were elucidated. The cell viability evaluated after 24 showed reduced time/concentration-dependent cell viability. At 19.8nM jararhagin concentration, there was a significant decrease in cell viability and pronounced morphological alterations such as loss of adherence in HEPA-1c1c7 hepatocellular carcinoma cells at the 186.2 nM jararhagin concentration.

Figure 7. Means ± standard deviation of the cell cycle phases of the HEPA-1c1c7 tumor cell of the Control Group and Jararhagin-treated Groups at concentrations of 128.7nM and 186.2nM.

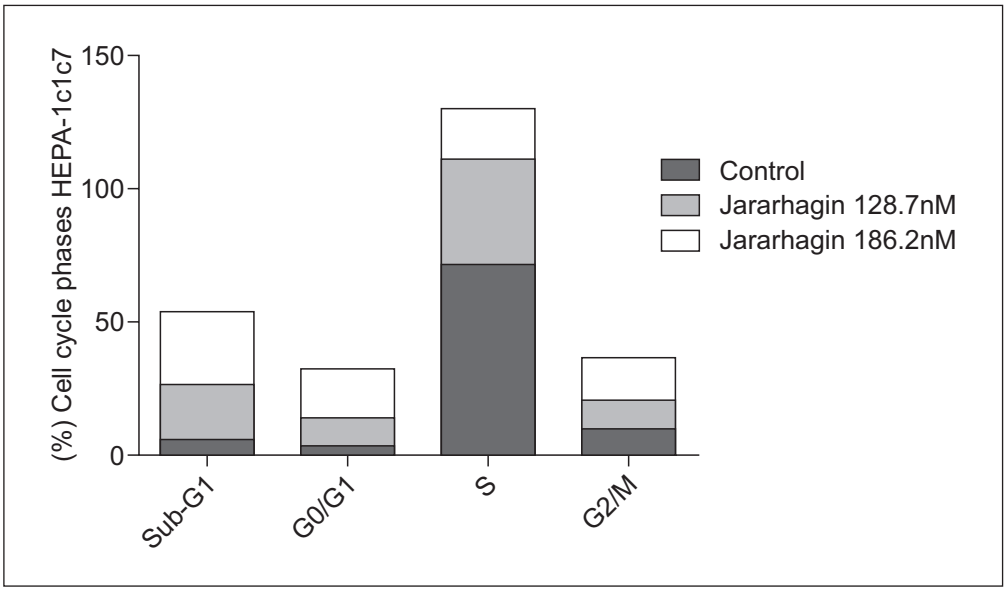

The number of experiments performed n=06. *Significant differences between the jararhagin-treated Groups and Control Group. ANOVA Variance Test followed by Tukey Kramer's Multiple Test. $p<0.001$.

MTT is a quantitative method, an indicator of mitochondrial metabolic activity, with a linear relationship between cellular activity and absorbance. Loss of membrane integrity often occurs after completing apoptosis in most of the cellular systems. Thus, treatment with jararhagin induced a decrease in mitochondrial activity at a concentration of 186.2nM in HEPA-1c1c7 tumor cells, and an increase in the percentage of inactive mitochondria, showing a cytotoxic effect of jararhagin.

In the process of origin of the lumen in cell culture, the selection of cells resistant to the anoikis process occurs, with the formation of cell groups and spheroids [15-16]. Spheroid growth is the result of aggregation, proliferation, polarization, adhesion molecule modulation, and lumen cell death [17,18].

Reactive oxygen species (ROS) are produced continuously in cells as by products of cellular metabolism, performing essential functions as mediators of protective mechanisms such as apoptosis, phagocytosis, and detoxification [18]. Excessive increase in ROS formation induces DNA damage, promoting mutagenic alterations of nucleotides, protein oxidation, and lipid peroxidation, playing a crucial role in tumorigenesis. Free radical-induced lipid peroxidation is a widely investigated process, and the cell membrane is one of the components most affected by the high concentration of polyunsaturated fatty acids susceptible to oxidation[19].

Oxidants, in general, produce protein modifications leading to loss of function and increasing the degradation rate of oxidized proteins, promoting changes in their structure and permeability, which leads to inhibition of cell growth and death. Lipid peroxidation may trigger the apoptosis process, activating the intrinsic apoptosis pathway present in all cells, whether or not dependent on the phosphorylation of the caspase pathway. Given the importance of the lipid peroxidation process in apoptosis, the results indicate that jararhagin dose-dependently affects this process, accompanied by cellular cytotoxicity and cellular morphological alterations, inducing

apoptosis, especially at concentrations below 1μM jararhagin in HEPA-1c1c7 tumor cells. There was also a decrease in the synthesis phase at both 128.7nM and 186.2nM concentrations, as well as an increase in G2/M and G0/G1 fragmented DNA. These data indicate that jararhagin is effective in reprogramming the cell cycle by inhibiting proliferation through synthesis inhibition.

The distinction between increased apoptosis or necrosis was assessed by the annexin V/PI labeling method by flow cytometry using the jararhagin treatment. Tanjoni (2005) demonstrated the induction of apoptosis with loss of cell adhesion, anoikis in jararhagin-treated endothelial cells, which indicates special attention to possible side effects on the vascular system [20].

There are several antiproliferative mechanisms, including apoptosis and senescence. Although senescence, similar to apoptosis, is also an extremely complex process, some forms of senescence are more precisely defined. Replicative senescence, which occurs in primary cells that are cultured *in vitro*, is dependent on telomere size and is usually reversed by telomerase expression. In recent years, however, it has become apparent that there is oncogene-induced senescence (OIS), which is activated by the activation of oncogenes such as Ras and Raf and requires p53, acting via CDK inhibitors, p21CIP, and p16INK. These two processes have irreversible arrest of growth and expression of beta-galactosidase in acid cell compartments in common, which allows the measurement of senescence. Senescent premalignant lesions were found in several normal tissues and are believed not to progress to malignancy due to senescence, indicating the importance of senescence as an antitumor process. This information, combined with the results obtained concerning p53 expression, demonstrates the participation of jararhagin concentration-dependent senescence and autophagy inducing mechanisms.

The ultrastructural microscopy images performed with the HEPA-1c1c7 tumor cells lineage obtained by confocal laser scanning fluorescence microscopy revealed at both concentrations a reduction in the number of morphologically viable cells, cell detachment, tumor parenchyma deconfiguration, cluster, and apoptotic body formation. While in the Control Group, an intense proliferation was observed with the formation of parenchymal structures. The expression of markers obtained in this lineage by confocal laser scanning fluorescence microscopy elucidated a significant dose-dependent increase in the expression of CD34 and CD44, glycoproteins involved in cell-cell interaction and function as an adhesion factor and cell migration, besides the considerable increase in activity of caspase-3, p53, and reduction in Cox-2 cyclooxygenase expression, actively involved in the process of tumorigenesis.

Scanning electron microscopy (SEM) showed hepatocellular carcinoma HEPA-1c1c7 cells cultured in monolayer and the extracellular matrix organization with many protrusions. Retractions and cell aggregates were observed at 128.7nM jararhagin concentrations. In cells treated with 186.2nM, there was the detachment of the plaque surface and formation of smaller aggregates, apoptotic bodies, and necrotic debris.

The sum of IC50 values, morphological alterations, and cell viability together suggest the possible use of jararhagin as an antitumor agent capable of inducing cell death. However, their toxicity in normal cells should be evaluated and redirected to other studies, such as site-specific nanocarriers to reduce the toxic effect in normal cells, as well as studies that elucidate the cellular signaling pathways involved in this process. After that it is possible to establish which are the inducers of necrotic and apoptotic death in normal cells, as they were done in the HEPA-1c1c7 hepatocarcinoma lineage, seeking to safely establish the use of this snake venom metalloproteinase in cancer therapy.

The HEPA-1c1c7 cells used in this study are murine hepatocarcinoma cells, and in jararhagin concentrations required for induction of IC50% cytotoxicity were very close on a monometric scale, causing morphological and inductive alterations of similar human cells death. This may

suppose an indication that murine cells, as well as human cells, are equivalently sensitive to the mechanism of action of jararhagin and can be used as efficiently as animal guinea pig models to prove the efficacy of this toxin *in vivo*.

Conclusion

Jararhagin-treated HEPA-1c1c7 murine hepatocellular carcinoma cells showed a reduction in the synthesis phase at both 128.7nM and 186.2nM concentrations, as well as an increase in fragmented DNA and arrestin G2/M. The expression of markers obtained in this lineage by confocal laser scanning fluorescence microscopy elucidated a significant dose-dependent increase in the expression of CD34 and CD44, glycoproteins involved in cell-cell interaction and that function as cell adhesion and migration factor, besides the considerable increase in activity of caspase-3, p53, and reduction of Cox-2 cyclooxygenase expression, actively involved in the process of tumorigenesis. Scanning electron microscopy (SEM) showed that HEPA-1c1c7 hepatocellular carcinoma cells underwent significant morphological alterations such as cytoplasmic retraction and aggregate formation, also showing detachment of plaque surface and formation of apoptotic bodies and necrotic debris.

References

1. Institute National of Cancer - INCA. Liver cancer. 2018. Available in: <https://www.inca.gov.br/tipos-de-cancer/cancer-de-figado> Access on: 24 nov. 2019.
2. Lopes FLM, Coelho FF, Kruger JAP et al. Influence of Hepatocellular Carcinoma Etiology in the survival after resection. ABCD Arq Bras Cir Dig, 2016; 29 (2); 4:105-108.
3. Balogh J, Victor D, Asham EH et al. Hepatocellular Carcinoma: A Review. Journal of hepatocellular carcinoma. 2016;3;13:41-53.
4. Caldwell S, Park SH. The epidemiology of hepatocellular cancer: from the perspectives of public health problem to tumor biology. J Gastroenterology. 2009; 44 (Suppl XIX);6:96-101.
5. Chedid MF. Hepatocellular carcinoma: diagnosis and operative management. ABCD Arq Bras Cir Dig. 2017; 30 (4); 7:272-278.
6. Institute Oncoguia. Liver Cancer survival rate. Available in:http://www.oncoguia.org.br/conteudo/taxa-de-sobrevida-para-cancer-de-figado/8295/208/> Access on: 21 nov 2019.
7. Ma R, Ravikiran M, Kwok H. Venon-based peptide therapy: insights into anti-cancer mechanism. 2017;8(59);23:100908-100930.
8. Ferreira BA, Deconte SR, Moura FBR et al. Inflammation, angiogenesis and fibrogenesis are differentially modulated by distinct domains of the snake venom metalloproteinase jararhagin. 2018;119;9:1179-1187.
9. Klein A, Capitanio JS, Maria DA, Ruiz IRG. Gene expression in SK-Mel-28 human melanoma cells treated with the snake venom jararhagin. 2011;57(1);8:1-8.
10. Rodriguez MGP. Evaluation of antitumor effects of ophidic metalloproteinase jararhagin in breast adenocarcinoma. 2012. 171 p. Masters thesis (Biothecnology) – Institute of Biomedical Sciences, USP. 2012;172:1-172.
11. Son DJ, Park MH, Chae SJ et al. Inhibitory effect of snake venom toxin from Vipera lebetina turanica on hormone-refractory human prostate cancer cell growth: induction of apoptosis through inactivation of nuclear factor kB. Mol. Cancer Ther.2007;6;9:675-683.
12. Moura-da-Silva AM, Marcinkiewicz M, Niewiarowski S. Selective recognition of α2 β1 integrin by jararhagin, a metalloproteinase desintegrin from *Bothrops jararaca* venom. Thrombosis Research. 2001;102;7:153-159.
13. Cimpeam AM, Ribatti D, Raica M. The chick embryo chorioallantoic membrane as a model to study tumor metastasis. Angiogenesis. 2008;11(4);9:311-319.
14. Correa MC, Maria DA, Moura-da-Silva AM, Pizzocaro KF, Ruiz IRG. Inhibition of melanoma cells tumorigenicity by the snake venom toxin jararhagin. Toxicon. 2002;40;10:739-748.
15. Simpson CD, Anyiwe K, Schimmer AD. Anoikis resistance and tumor metastasis. Cancer Lett. 2008;272(2);9:177-185.
16. Kenny PA, Lee GY, Myers CÁ et al. The morphologies of breast cancer cell lines in three-dimensional assays correlate with their profiles of gene expression. Mol. Oncol. 2007;1(1);13:84-96.
17. Do Amaral JB, Urabayashi MS, Machado-Santelli GM. Cell death and lumen formation in spheroids of MCF-7 cells. Cell Biol. Int.2010; 34 (3);8:267-274.
18. Li Q, Sato EF, Kira Y et al. A possible cooperation of SOD1 and cytochrome c in mitochondria-dependent apoptosis. Free Radic. Biol. Med. 2001;40(1);8:173-181.
19. Sodergren E. Lipid peroxidation *in vivo*. Evaluation and application of methods for measurement. Ph. D. thesis (Medical Science in Geriatrics) Comprehensive Summaries of Uppsala Dissertations from the Faculty of Medicine, Uppsala University, Scandinavia. 2000;78:1-78.
20. Tanjoni I, Weinlich R, Della-Casa MS et al. Jararhagin, a snake venom metalloproteinase, induces a specialized form of apoptosis (anoikis) selective to endothelial cell. Apoptosis. 2005;10;11:851-861.

Humanoid Prototype Development Through 3D Printing for New Technologies

Matheus Henrique Nunes França[1]*; Fredson da Silva Oliveira[2]; Oberdan Rocha Pinheiro[3]
[1,2]Wyden, Engineering; [3]SENAI CIMATEC, Department of Robotics: Salvador, Bahia, Brazil

Robotics creates the possibility of using robots to assist humans in several tasks, especially in hostile environments to humans. In order to cope with different types of environments, it is of great importance that robots are adaptable to the environment in which they operate. So, this study aimed is to develop a prototype of a humanoid robot by 3D printing as close as possible to the human being. The prototype will be used as the cradle of tests and thus will advance the most diverse techniques in robotics and artificial intelligence.
Keywords: Humanoid. 3D Printing. Robotics.

The growing interest in humanoid robots has substantially helped to increase their development over the past decade. The existing humanoids can be classified as wheeled humanoids, legged humanoids, and human-like [1]. This research project offers an open-source humanoid model, printed in 3D. In particular, the use of 3D printing technologies and rapid prototyping is a central aspect of this project and makes it easy and fast, reproducing the platform, and also exploring its use in science and education. The project was initially designed with a scientific objective, aiming to be an experimental platform, opening the possibility to systematically study the role of morphology in motor sensor control in human-robot interaction and cognitive development.

Methods

The conception of the humanoid robot takes into account all human anthropomorphic characteristics. In this sense, it was built with hybrid performance, designed to assist the motors aiming to improve energy efficiency when moving their joints. The design was developed with the aid of Fusion 360 software, while the parts were manufactured using a 3D printer. Seventeen LOBOT LX-16A servo motors, an Xbox 360 Kinect Sensor, a raspberry pi 3, 7 mpu6050 gyros, and 8 Sparkfun 5" force sensors were used, which are the elements that comprise the prototype. Following is a description of the steps for building the prototype.

Received on 18 October 2019; revised 23 September 2019.
Address for correspondence: Dr. Matheus Henrique Nunes França. Avenida Orlando Gomes, N. 1845, Piatã. Zip Code: 41650-010. Salvador, Bahia, Brazil. E-mail: br_matheus@hotmail.com. This study was selected from the V International Symposium of Innovation and Technology - SIINTEC (October 2019). DOI: https://doi.org/10.34178/jbth.v2i4.90

J Bioeng. Biotech. Appl. Health 2019;2(4):123-129.

Active and Passive Action

One of the significant challenges of the project was to develop human-like walking and sturdiness when in the presence of disturbances, such as variations' terrain [2]. The main problems associated with the analysis and control of bipedal robots are changes due to the impact of the leg on the ground. These issues required a sturdy structure that minimizes engine stress. Two categories of biped robots were analyzed: 1) Operating performance: Biped robots that have feet and actuators in some of the joints (the performance is made in such a way as to take advantage of the natural characteristics of walking); and 2) Passive performance: Purely passive biped robots without feet and torque or position control.

Structure Dimensioning and Servo Motors

Structure

The robotic structure has actuators that give them diverse degrees of freedom [3] needed for natural motion. For each joint, a motion study was needed to know how many engines would be inserted. For each GDL, an actuator is required;

thus, the structure sizing depends on how many motors will be inserted. However, to determine the motors, it is necessary to have parameters such as the weight and size of the structure. It follows that the design of the structure and actuators are directly related, so we chose to make a constraint in which to make decisions. The delimitation of the structure was made, choosing a small structure, but not losing the characteristics of the human being. So, the maximum dimension of 1 meter was chosen. After the choice, it was only necessary to make a scale with the human body and then get the dimensions necessary to start the project. With the delimitations made in the structure, the engine could start being detailed.

Servo Motors

The servo (actuator) chosen for the project works with a servo mechanism that uses position feedback to control the speed and final position of the motor. Internally, a servo combines a motor with a feedback circuit, a controller, and other complementary circuits. It uses an encoder or speed sensor (encoder) that has the function of providing speed and position feedback. The servo chosen was the lobot LewanSoul LX16-A, which has as parameters the speed and position feedbacks already mentioned, as well as temperature and voltage for greater control, and also a torque and a small dimension.

Computer Assisted Drawing (CAD) and Structural Analysis

A complete study of the human body was necessary. The technic design, which was part of the project, started with the sizing of the structure and the chosen engine. The design was done in the Fusion 360 software. For the freedom of movement tests that the body would have, we corrected all errors. The model was used for production in the 3D printer. After the design finished, it was processed by the 3D printer program, in which case Simplify 3D generated the machine code (g code), and, thus, made the part itself.

Foot

The project was started by simplifying the toes because of their complexity, but not compromising the march, so the foot only needed one axis of rotation for the toes. The feet (Figure 1) also included a set of force sensors for ground impact analysis and a sensor (mpu6050) containing gyroscope, accelerometer, and temperature capture. Rubber soles were used to avoid slipping on smooth surfaces. It was necessary to insert four cavities for the coupling of force sensors and a mechanical limit switch on the finger so that it did not exceed 45º hyperextension.

Ankle

One actuator coupled to the foot, one to the ankle, and the other just above, to the shin to accommodate the three-foot movement actuators allowing to maximize gaps (Figure 2).

Shins

The shin (Figure 3) accommodated both the foot and knee movement motor, which resulted in space optimization in the humanoid. Other gyroscope was also placed on this limb for movement analysis, and we also inserted tubes to stiffen the structure.

Knee

In the knee, only a degree of freedom was needed; thus, the system was simple than in the ankle. As already mentioned, the engine was housed in the shin. Its transmission was made directly on the motor shaft, which maintains a ratio of 1:1 not to change its torque or speed. Despite its simplicity, the knee is a joint much demanded by the robot's structure (i.e. [4]). The structure, like the toe, also has a mechanical limit switch that limits the structure to its flexion, leaving aside unnecessary hyperextension.

Thigh

The thigh (Figure 4) was divided into two parts, the first part coupled to the knee including the

Figure 1. a) Top view of the foot with silicone (mechanical end of stroke). b) Bottom view of the foot without silicone (showing cavities for sensors).

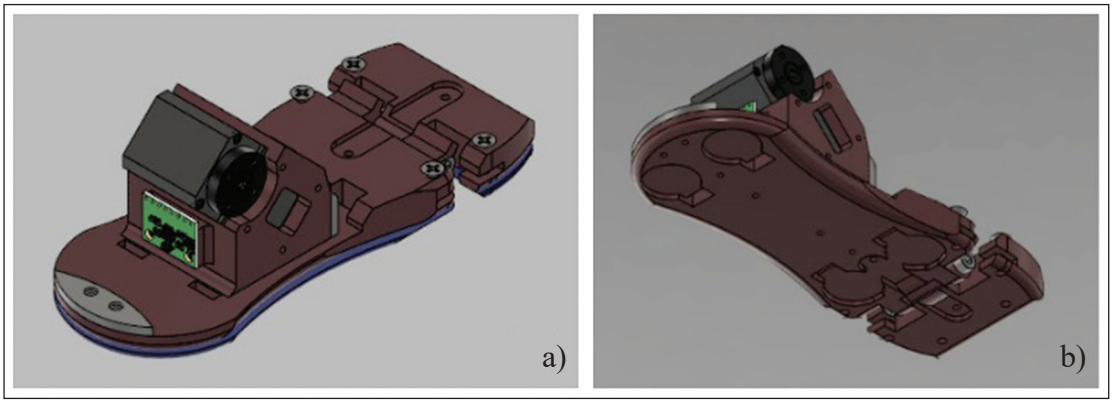

Figure 2. a) Ankle front view. b) Ankle connected to the foot.

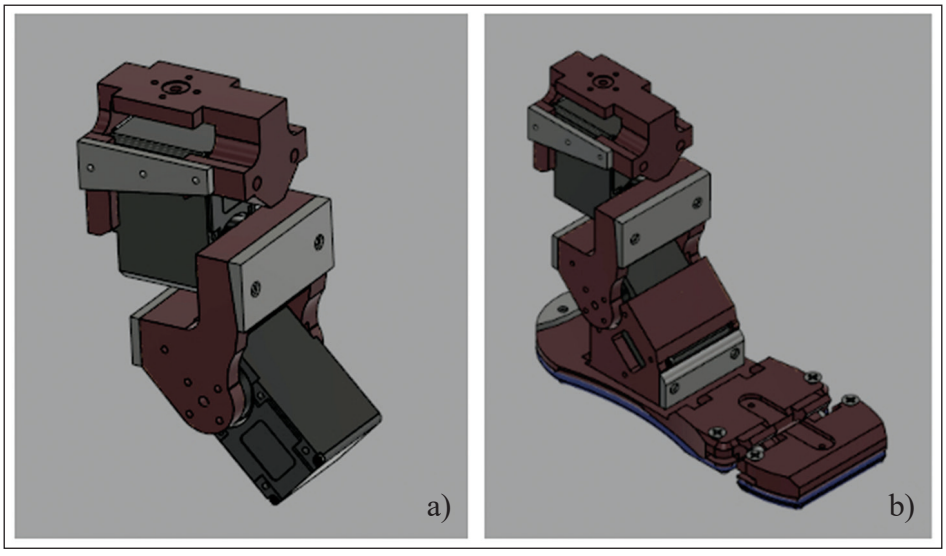

gyro sensor, structural fortification tubes, and the lateral and medial rotation motor of the hip or the thigh. The second part comprised the hip ligament that makes the abduction and hyperabduction movements.

Hip

The hip (Figure 5) must have 3 degrees of freedom for the leg and 1 degree of freedom for the trunk.

The motor shafts are connected to the structure in a cascade, which, although not anthropomorphically correct, does not affect its expected final movement. Since this is a large part of the robot's structure, it had to be divided into three parts. The first had the trunk rotation motor, and the other two connected the central part with the thigh joint. Cylinders were also placed to increase its strength and a bearing to aid in body torso movement.

Body Torso

The body torso (Figure 6) contained 3 degrees of freedom, and like the other joints of

Figure 3. a) Front view of the shin already attached to the knee. b) Back view of the shin.

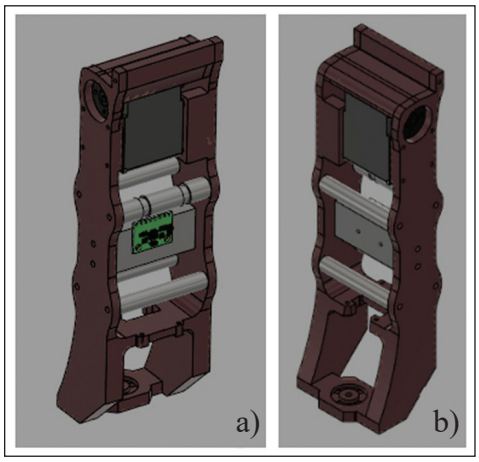

Figure 4. Thigh with all parts assembled in fusion 360 software.

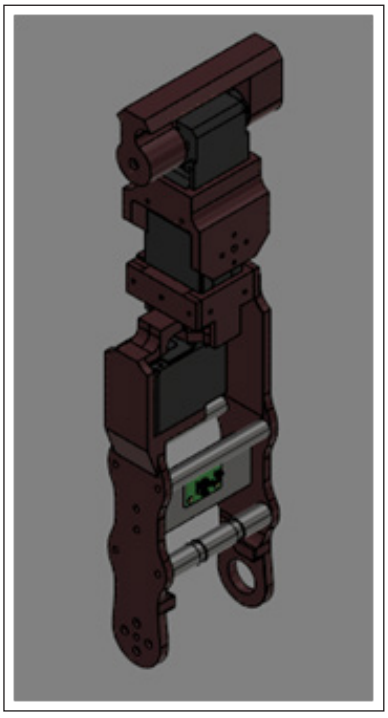

Figure 5. a) Hip in front view. b) Hip in back view with servo showing.

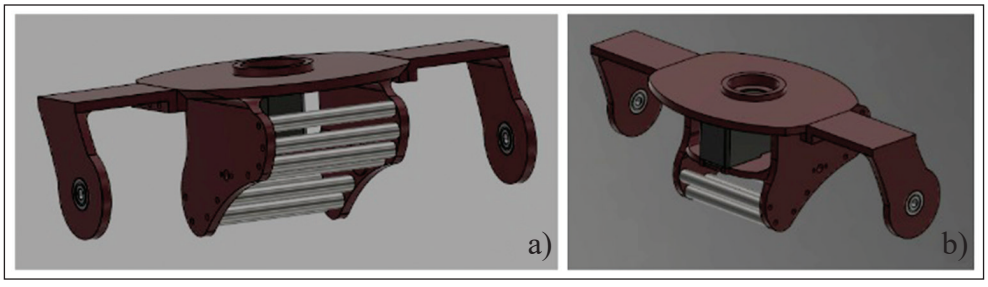

the structure, it was connected in cascade. The rotational movement was inserted into the hip. The body torso accommodated the central part of the electronics. It had a gyroscope, the buslinker card for the servo, the raspberry pi 3 for the control part, and contained speakers, an LCD screen, and a Kinect on top.

Structure Production

A very satisfactory solution was designed after the humanoid drawings were made, accommodating a total of 19 degrees of freedom (2 of them purely passive, Table 1) and the dimensions of a human being approximately 1 meter high. This solution meets all the requirements imposed at the beginning of this study regarding measurement and handling.

Table 1. Distribution of DoF's (Degrees of Freedom) of Adam's Humanoid Robot.

Joint	DoF's Number
Foot	1(x2)
Ankle	3(x2)
Knee	1(x2)
Hip	3(x2)
Body Torso	3
Total	19

For the construction of this structure, the 3D Anet A8 printer was used because it has a low production cost and an excellent technical quality. It used the filament petg xt, which is a material of high mechanical, chemical and temperature resistance, hardness, and neutral odor of processing. The PETG is a durable copolyester. The PET, think of bottle plastic, and G of glycol modified for extra durability. We began printing the parts by the foot, which consisted of two parts and the four parts that composed the silicone mold, followed by all the other parts that made up the right leg and the hip, only then started the left leg and the body torso. After finishing the 3D printing and the assembly, we started to place the passive actuators, and, in this case, rubber bands were used. Then, the sensors and all the electronics were placed, and just then, the plates covering the entire structure were installed.

Results and Discussion

The structural design (Figure 7) was developed in a 3D printer with an environmentally friendly material, initially built the part of the robot's body torso and legs. In future work, the upper limbs and the head will be structured. All movements have reached the required amplitudes for the desired structure as well as the desired size. The passive

Figure 6. a) Body torso with lid containing the LCD. b) Trunk with part of the visible electronics.

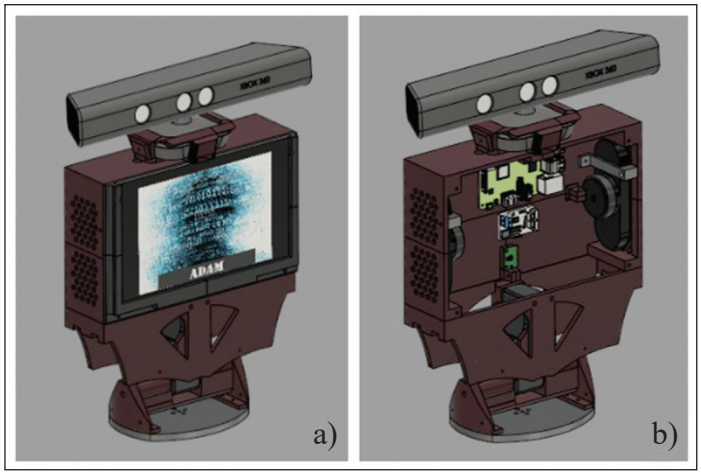

actuators that assist the servo motors have been assertively inserted. A mechanical loss was observed in the most demanded actuator connections due to the structure is made of copolyester and not of a stronger material such as aluminum. This results in much faster wear on the movement axes, causing a lag in movement angles.

Conclusion

Robotics has been driven by the possibilities of using robots to assist humans in several tasks. In order to cope with different types of environments, it is of great importance that robots can develop mobility strategies that are adaptable to the environment in which they will operate. In this sense, our humanoid prototype aimed to generate a cradle of tests in which researchers in the field of robotics can develop their studies, thus bringing an enriching possibility of knowledge sharing, and accelerating the development in this area of this field. Another possibility for humanoids is the insertion in schools in order to increase students' interest in this area.

At first, a platform was created, which consisted of legs, body torso, and the computer vision part with Kinect. Every prototype made in a 3D printer uses both active acting (with motors) and passive acting (rubber bands) in their joints. We also used sensors to capture maximum feedback from the outside world. As future research work, the development of intelligent deliberative agent-

Figure 7. a) View without protection plates. b) View with protective plates. c) The structure already machined and with passive actuator.

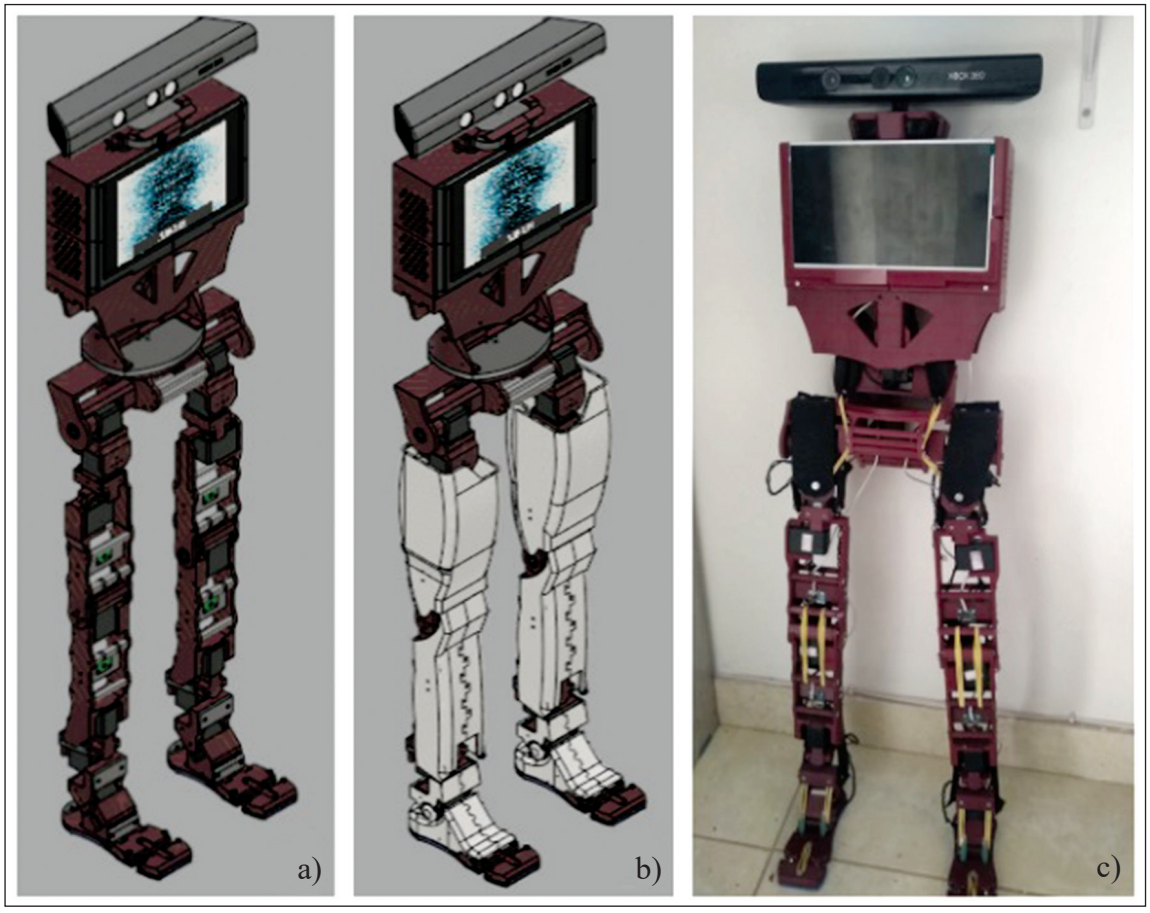

based stability and walking control using advanced machine learning techniques is suggested.

References

1. Bar-Cohen Y et al. The Coming Robot Revolution; Springer: Berlin, Germany; Heidelberg, Germany, 2009.
2. Sariyildiz E, Temeltas H. Turkish Journal of Electrical Engineering & Computer Sciences. 2017;25(2):1495-2.
3. Lida F, Minekawa Y, Rummel J, Seyfarth A. Toward a human-like biped robot with compliant legs. Robotics and Autonomous Systems. 2009;57:139-144.
4. Lahr DF, Yi H, Hong D. Advanced Robotics. 2016;30(2):109-118.

Mathematical Modeling of the Extraction Process Essential Oils *Schinus terebinthifolius Raddi* Using Supercritical Fluids

Ana Carolina Araújo dos Santos[1]*; Gabriel Antônio Batista Nascimento[1]; Natália Barbosa da Silva[1]; Victor Laurent Sampaio Ferreira[1]; Yan Valdez Santos Rodrigues[1]; Ana Lúcia Barbosa[1]; Ewerton Emmanuel da Silva Calixto[1]; Fernando Luiz Pellegrini Pessoa[1]

[1]Centro Universitário SENAI CIMATEC; Salvador, Bahia, Brazil

***Schinus terebinthifolius Raddi* is a plant rich in nutrients and is used medicinally and industrially. Supercritical oil extraction from *S. terebinthifolius* can result in higher value-added products. Mathematical models (Sovová and Esquível) are used to describe the behavior of supercritical extractions. This study aims to compare both models in terms of yields in conditions of 223 bar and 50°C. We observed that the model proposed by Sovová provided good reproducibility and representativeness.**

Keywords: *Schinus terebinthifolius Raddi*. Supercritical Extraction. Esquivel. Sovová.

Brazil has abundant plant species with great economic and medicinal potential. Aroeira (*Schinus terebinthifolius Raddi*) is one example of a nutrient-rich plant, which is used both medicinally and industrially due to the chemical components and carotenoids.

Several extraction methods of essential oils can be used. However, one of the most promising is supercritical extraction because it leaves no trace of the solvent in the product, has excellent quality and also because environmental legislation prohibits waste of solvents in industrial processes. According to Brunner [1], no substance is a supercritical fluid, but it can become one by increasing heat and pressure beyond the critical point.

Thus, a supercritical fluid is a pure fluid above such characteristics. The most used solvent in this type of extraction is CO_2. It's safer and has a lower cost when compared to other fluids that are usually expensive or have low access or leaves waste after extraction.

Received on 23 September 2019; revised 10 October 2019.

Address for correspondence: Dr. Ana Carolina Araújo dos Santos. Centro Universitário SENAI CIMATEC. Av. Orlando Gomes, 1845, Piatã. Zip Code: 41650-010. Salvador, Bahia, Brazil. E-mail: anacarolina28160@gmail.com. This study was selected from the V International Symposium of Innovation and Technology - SIINTEC (October 2019). DOI: https://doi.org/10.34178/jbth.v2i4.91

J Bioeng. Biotech. Appl. Health 2019;2(4):130-135.

Sovová's model [2] considers that the material to be extracted contains intact innercells and the outer cells are ruptured, wrapped in a spherical greenhouse. It also takes into account the solvent-solute balance inside the cell during pressurization, with the concentration unchanged in the intact cell [3].

Esquivel [4] proposed a model in order to expose the extraction curves that are easily modeled using an empirical equation for the experimental curve fit, and this empirical model does not consider solute-matrix interactions [5]. This paper aims to compare oil extraction yields provided by the mathematical models proposed by Sovová and Esquível [2,4] for the oil extraction of *Schinus terebinthifolius Raddi*.

Methods

Data and Tools

The data used herein is related to an extraction process performed at 223 bar and 50°C. The Microsoft Excel Solver® was used to carry out the calculations, and the curves were plotted in a Microsoft Excel spreadsheet.

For modeling the extraction curves of *Schinus terebinthifolius Raddi* oil, two mathematical models were used: Sovová [2] and Esquivel [4].

Both require the proper determination of process variables and parameters, such as solvent density,

particle density (ρS), particle diameter, solubility, bed porosity (ε), bed height, and extractor radius obtained for the condition of interest (223 bar and 50°C). Table 1 presents the experimental data.

Table 1. Experimental data used for extraction curve modeling.

Temperature	323.15 K
Pressure	220.08 atm
QCO_2	23.13 mL/s
ε (Porosity)	0.3231
Rs	0.50 g/mL
Dp	0.00168m
rCO_2	0.84 g/mL
Bed height	0.24400 m
Solubility	3.40 Kg solute/ m^3 solvent
Bed diameter	0.01350 m
Solvent flowrate	1.38775 L/min
Sample mass	10.00310 g
%(w)solute	3.9804
%(w) solute inaccessible	30.83
elim	3.98
Cross-sectional area	0.00014 m^2
Solvent molar mass	44 g/gmol
Sample solute mass	0.39817 g
Solute free sample mass	9.60493 g
Solute inaccessible mass	0.12277g

Extraction Curves

A typical extraction curve consists of three regions (Figure 1).

Each region is characterized by the predominance of one or more mass transfer phenomena. The first part of the curve is a straight line that indicates a constant extraction rate, i.e., governed by convective mass transfer between the surface of the solid and the solvent.

The next region is a transitional, where the extraction rate drops rapidly as soon as a change from the convection predominates over diffusion, where the later control mass transfer and the slope of the curve decreases and becomes asymptotic [1].

Sovová's Model [2]

This model considers a pseudo-steady state, in which the temperature, pressure, and solvent velocity are kept constant. There is an axial flow of the solvent with superficial speed through a fixed bed of cylindrical cross-section, and the solute is inside the plant cells. We also assumed that pretreatment of the material, such as grinding, which increases the contact surface between solid and solvent, separates the total amount of available solute into two parts, one of easy access and other of difficult access. Each extraction curve region was determined using the following equations [2]:

$$CER = \left(\frac{X_k \tau}{Z}\right)(1 - e^{-Z}) \quad \tau < \tau_m \qquad (1)$$

$$FER = \left(\frac{X_k}{Z}\right)\left(\tau - \tau_m e^{(Z_w - Z)}\right) \quad \tau \leq r < \tau_n \qquad (2)$$

$$DC = X_0 - \left(\frac{X_k}{KZ}\right)\ln\left(1 + e^{(r_0 KZ)} - 1\right)\frac{e^{(K(\tau_m - \tau))}}{r_0} \quad \tau > \tau_n \qquad (3)$$

For instance, τ is the criterion to define the dominant region in a specific time interval of the extraction process.

Esquível's Model [4]

Monod model uses the microbial growth kinetic equation proposed to represent the microbial extraction yield as a function of extraction time [5]. This model describes the extraction curves, however, it does not consider the solute and solid matrix interactions. It is simpler than Sovova's model [2], with only two parameters to be determined [6]. The following equation describes it:

$$e = e\_lim\ (t/(b+t)) \qquad (4)$$

The character "e" is the ratio of the mass of oil recovered in time t(s) and e_limis the e value for infinite extraction time.

We did a a regression with the experimental data, and the parameters that gave the maximum yield and minimum error were determined.

Figure 1. Extraction curve with two straight lines adjusted.

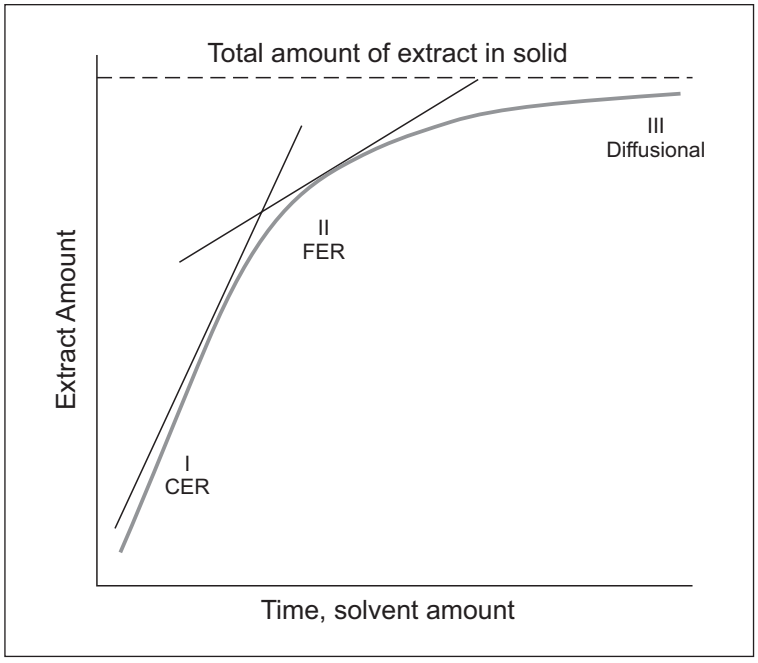

CER: Constant Extraction Rate Stage - transfer predominance mass due to fluid phase convection. FER: Falling Extraction RateStage - convective effects on stage fluid, and solid-phase diffusions determine the speed of the process. DC: Almost Zero Extraction Rate Stage - the predominance of diffusional effect.

Results and Discussion

The great extraction' yield was obtained at 50°C 223 bar (Sovová model) (Figure 2), diferently from Esquível model [4] (Figures 3, 4). At the same condition, the curve presents precisely the behavior described by Sovová in the CER region, passing through a transition range until it stabilizes at a particular value (elim).

The beginning part of the curve represents a line that indicates a constant oil extraction rate. At this time, a surface oil layer surrounds the solid matrix particles. At this point, the extraction is characterized by convective mass transfer between the surface of solid and solvent. The constant extraction rate region follows a transition stage, during which the extraction rate drops rapidly. Therefore, the diffusional process begins to control the mass transfer, as the solvent finds free space for the penetration in the matrix, product solubilization, and subsequent diffusion of the oil-solvent mixture to the particle surface.

Almost no extraction performed in the last region. At this level, the slope of the curve decreases, and the plot approaches the value that represents the theoretical content of the extractable oil of *Schinus terebinthifolius Raddi* [2].

In addition, the parameters kf (fluid-phase mass transfer coefficient), Z (fast extraction period parameter), W (slow extraction period parameter), Yr (solubility) and ks (solid-phase mass transfer coefficient) were generated for the model Sovová [1] and estimated for the previous conditions using regression analysis to minimize the square of the difference between the experimental values and calculated by the model. Mass transfer coefficients of the solid and fluid phases were calculated from these parameters. For instance, the parameter Xk

Figure 2. %Yield (Experimental and model based on Sovová [2,3]).

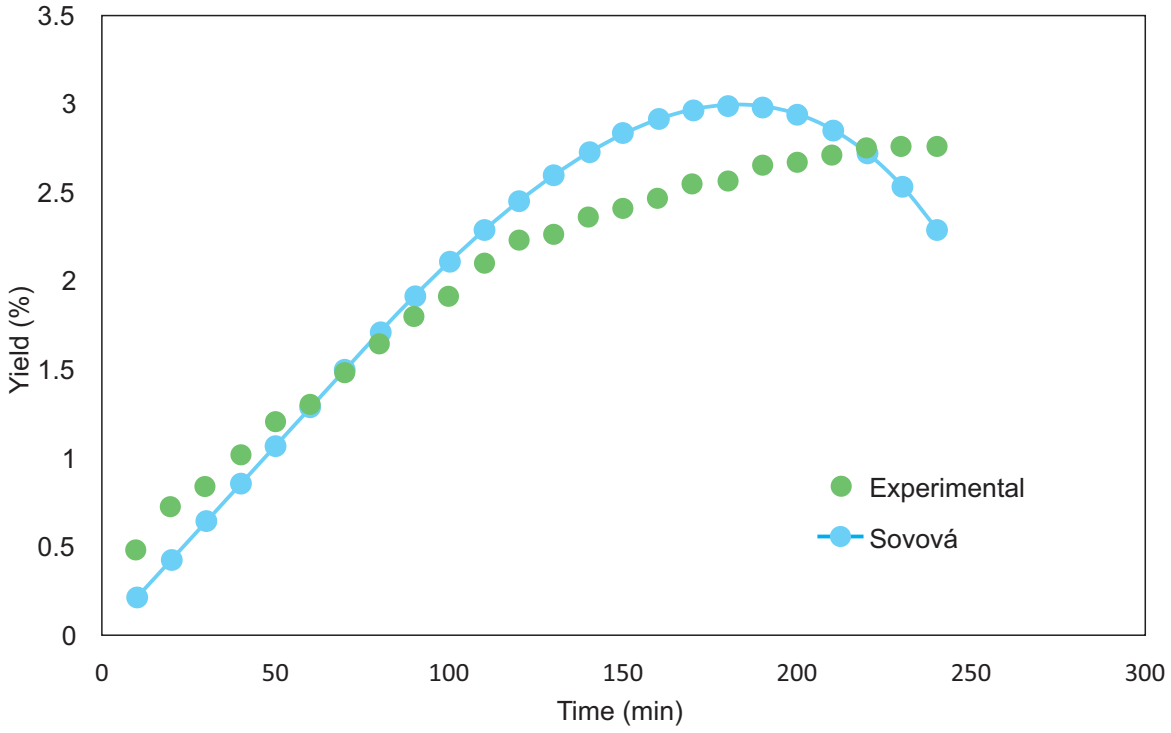

Table 2. Estimated parameters and mass transfer coefficients.

Xk	Z	W	yr	kf (m/s)	ks (m/s)
0.013	1.296	0.059	0.0088	0.0004	0.0009

Table 3 presents the algorithm parameters determined by the regression according to the Esquivel model [4].

Table 3. Parameters from the linear regression of the experimental curve.

b (calc)	59.11
e_{lim} (calc)	3.04
Equation	*e*= 3.039 (t/(59.1134 + t)

New parameters needed to be estimated due to the existence of residuals in the calculation of the model (Table 4).

Table 4. New parameters.

b (calc)	104.13
e_{lim} (calc)	3.98
Equation	*e*= 3.9804(t/(104.1301 + t)

Figure 3. Experimental *vs*. simulated data using Esquivel model [4].

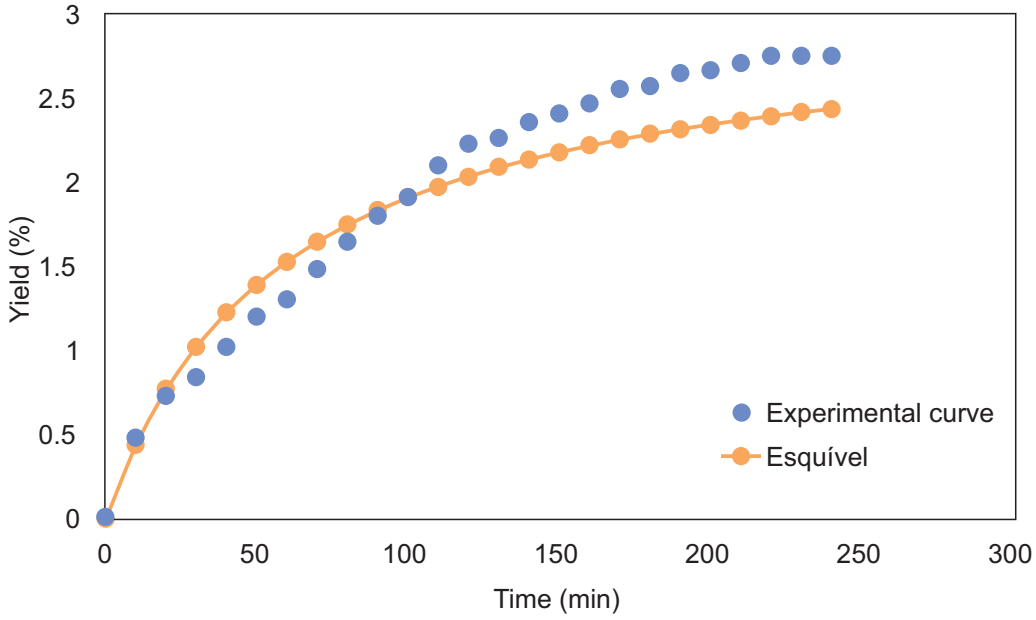

Figure 4. Experimental *vs*. simulated data through corrected Esquivel [4].

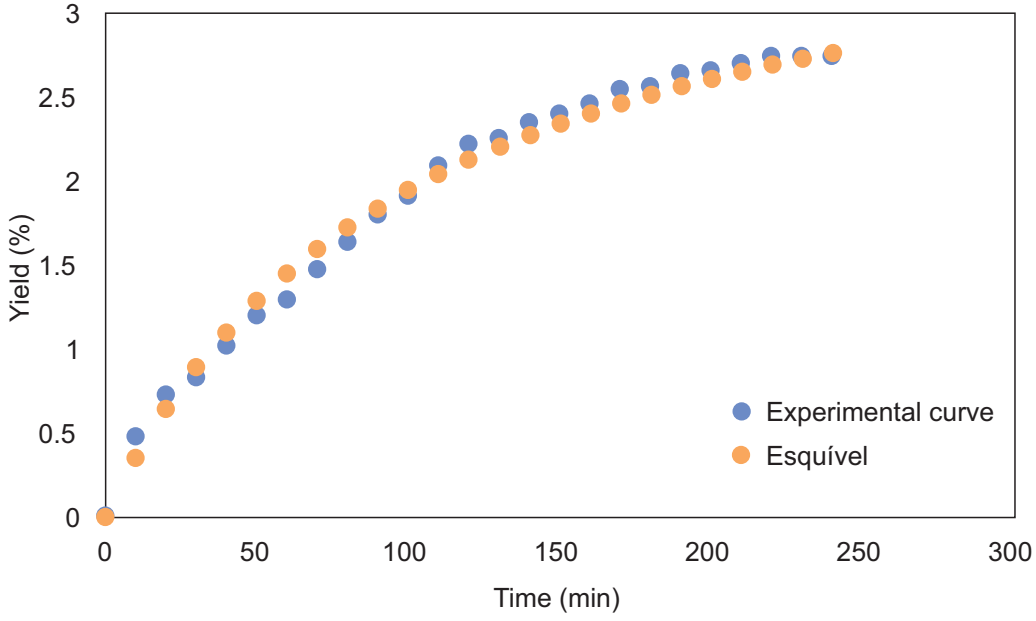

(inaccessible solute mass within the solid phase particles) presented the lowest values. So, most of the solute has been extracted by the previous two phases. Table 2 shows the mass transfer coefficients for the pressure of 223 bar and 50°C.

Conclusions

The present study allowed an analysis of the extraction curves of *Schinus terebinthifolius Raddi* (Aroeira) oil using two mathematical models [2,4]. Subsequently, the figures observations concluded

that Sovová's model has a higher yield than the experimental one. After 150 minutes, Sovová curve surpasses the experimental curve, due to the constant oil extraction rate. However, the values are not discrepant, having a small margin of error. Esquivel's mathematical model is less accurate since it is a simplified model using only two parameters, neglecting the axial and radial dispersions.

Therefore, the most accurate *Schinus terebinthifolius Raddi* oil extraction curve under conditions of 223 bar and 50°C, is that presented by the Sovová model.

Acknowledgment

We are grateful to the Professors Ana Souza, Ewerton Calixto, Fernando Pessoa for the opportunity to be part of this project, and to SENAI-CIMATEC University Center for the structural and technological support.

References

1. Brunner G. Gas extraction: an introduction to fundamentals of supercritical fluids and the application to separation processes. vol. 4. Springer Science & Business Media; 2013.
2. Sovová H. Mathematical model for supercritical fluid extraction of natural products and extraction curve evaluation. J Supercrit Fluids 2005;33:35–52. doi:10.1016/j.supflu.2004.03.005.
3. Sovová H. Rate of the vegetable oil extraction with supercritical CO2—I. Modelling of extraction curves. ChemEngSci 1994;49:409–14. doi:10.1016/0009-2509(94)87012-8.
4. Esquível MM, Bernardo-Gil MG, King MB. Mathematical models for supercritical extraction of olive husk oil. J Supercrit Fluids 1999;16:43–58. doi:10.1016/S0896-8446(99)00014-5.
5. Monod J. The Growth of Bacterial Cultures. Annu Rev Microbiol 1949;3:371–94. doi:10.1146/annurev.mi.03.100149.002103.
6. Bessa D, Souza ALB, Derner RB, Mendes MF. Modelagem matemática da extração de óleos bioativos de microalgas usando fluido supercrítico. 2015. doi:10.5151/chemeng-cobeqic2015-111-32296-264358.

Impact on Human Health of Particulate Matter Arising from Atmospheric Pollution

Clara Rodrigues Pereira[1]; Lílian Lefol Nani Guarieiro[2*]

[1]Centro Universitário Senai Cimatec, Master's degree course on Sustainable Development; [2]Centro Universitário Senai Cimatec, Integrated Campus of Manufacturing and Technology; Salvador, Bahia, Brazil

Studies show that exposure to particulate matter (PM) from vehicular combustion processes can pose severe risks to human health since the impact degree of PM on the respiratory system will depend on its size and composition. Thus, the objective of this study was to perform a systematic review on this topic, searching information that can highlight causes and solutions that may allow a greater understanding of this problem. We concluded that China is a country that stands out in the number of deaths caused by the emission of PM, given a highly polluted urban scenario. Besides, fine particles (PM2.5) are the most recurrent incidence of respiratory disease, as they are emitted mainly by industrial activities and vehicular emissions.

Keywords: Particulate Matter. Human Health. Respiratory System. Vehicle Emissions.

The global-technology-development evolution of urban cities contributes to the increase in air pollution. This situation calls attention to many organizations that look for actions that can reduce air pollution, such as the United Nations. It presented the 17 goals to improve the world in a time delta to meet them by 2030. This primary mission is to put into practice actions that can lead to the end of poverty, the prosperity and well-being for all, protect the environment, and face climate change [1]. Within this scenario, Goal 7 (Affordable and Clean Energy) stands out, as it shows measures to reduce significant pollution sources in the external environment, such as the participation of renewable energy in the global energy matrix and access to clean energy technologies [1].

In this scenario, substances that are emitted by industries, car exhausts, and other urban activities are deposited on road pavements and in human circulation spaces [2]. These factors contribute to the increase of air pollution and exposure of the individual to this environment [2]. Data from the World Health Globalization (WHO), in 2016, showed that air pollution in cities and rural areas is responsible for 4.2 million premature deaths per year due to exposure to particulate matter (PM), which causes cardiovascular, respiratory and carcinogenic diseases [3]. This information shows the level of impact that the PM can have on human health. But why? What causes these particles to damage our bodies? How are they formed, and what is their origin?

Atmospheric PM consists of mixtures of airborne solid particles that vary in size and chemical composition. They can be comprised of nitrates, sulfates, organic and elemental carbon, organic compounds, biological compounds, and metals (iron, copper, nickel, zinc, and vanadium) [4]. They derive from natural sources, which do not involve human activities (sea salt particles, windblown sand, volcanic ash), and anthropogenic sources, which come from urban processes (industrial processes, vehicles, and fuels) [5].

The length of the aerodynamic diameter of PM is the main factor that determines the capacity of particle transport in the atmosphere and the penetration capacity in the human respiratory system [4]. The PM can be classified into three groups: Coarse particles (PM10), which include diameter sizes between 2.5 and 10 μm, fine particles (PM2.5) with a diameter less than 2.5 μm, and ultrafine particles (PM0.1) with diameter less than 0,1 μm [4]. Coarse particles (PM10) are defined as primary particles once they are directly emitted

Received on 25 September 2019; revised 28 October 2019.
Address for correspondence: Dr. Lílian Lefol Nani Guarieiro. Centro Universitário SENAI CIMATEC. Av. Orlando Gomes, 1845, Piatã. Zip Code: 41650-010. Salvador, Bahia, Brazil. E-mail: lilian.guarieiro@fieb.org.br. This study was selected from the V International Symposium of Innovation and Technology - SIINTEC (October 2019). DOI: https://doi.org/10.34178/jbth.v2i4.92

J Bioeng. Biotech. Appl. Health 2019;2(4):136-140.

into the atmosphere [4]. Fine particles (PM2.5) are classified as secondary since their formation in the atmosphere occurs through chemical reactions [4].

The emission of particulate matter plays a prominent role in the literature by showing severe diseases that may be caused by the impact of PM on the respiratory tract, such as cardiovascular diseases, respiratory diseases, and diseases of the nervous system [2]. Therefore, some monitoring ways are already being adopted to identify the level of PM emitted by urban activities [3]. They can be fixed or mobile stations that have adequate tools to define which sizes are most emitted and their emission source [3]. However, it is vital for the evaluation of human exposure to PM and its impact on them. Thus, mathematical modeling aimed at simulating MP deposition in the lung is one of the critical tools in assessing its impact on health [6].

So, the main goal of this study was to accomplish a systematic review on the impact of particulate matter on human health when emitted by urbanization processes.

Method

The method applied for the development of this study was the systematic review (Figure 1). This method was developed according to the following steps: i) the keywords used were "particulate matter", "dry deposition", "wet deposition", "vehicular emission", "lung deposition"; ii) the databases used for research were Scopus (www.scopus.com), Science Direct (www.sciencedirect.com) and Capes (www.periodicos.capes.gov.br); iii) the established search period was from 2009 to 2019; iv) we verified if the title of the articles had the determined keyword; v) the abstracts were read according to the established filter (Figure 1).

Results and Discussion

One of the steps used in the systematic review was the time interval (2009 to 2019) stipulated in the search for materials related to the theme presented. Therefore, Graphic 1 represents how the study concerned has evolved over the years, proving that the theme has drawn attention, presenting a high degree of importance (Total of 120 articles).

From the systematic review performed in this study, it was possible to direct the research to the impact that the MP, arising from urbanization processes, can have on human health. One hundred twenty articles relevant to the theme were obtained. Through the selection of studies, the countries that researched this problem the most were identified (Graphic 2).

China presented 40% of the articles selected for the study, which highlight the impact of PM on the health of individuals (Graphic 2). The main reason for this happens because of the air pollution in China, which has become the fourth significant health risk in all the world, presenting PM as the central air pollutant [7].

The high degree of pollution in China is recurrent from rapid urbanization and economic development, where most PMs are emitted by anthropogenic activities (industrial activities, vehicle emissions) [7]. Thus, exposure to this particulate represents a vulnerability in human health when deposited in the respiratory tract once the high levels of aromatic polycyclic metals and hydrocarbons are part of PM [7].

Figure 2 ratifies this statement by presenting an illustrative map, which shows data from the year of 2016 on what in each country, the highest lung mortality rates from inhalation of PM are evidenced. On the map, China has a mortality rate between 1500 and 1999 million, with the exact value of 1,830 million deaths caused by PM emission [8].

Exposure to PM is influenced by local conditions such as weather, seasons, topography, particle sources, and others. However, inhalation is the most important way for the human body to contact PM. Its degree of impact is related to the particle size deposited in the respiratory tract [9]. The deposition of PM in the lung occurs in a way

Figure 1. Flowchart of the systematic review method.

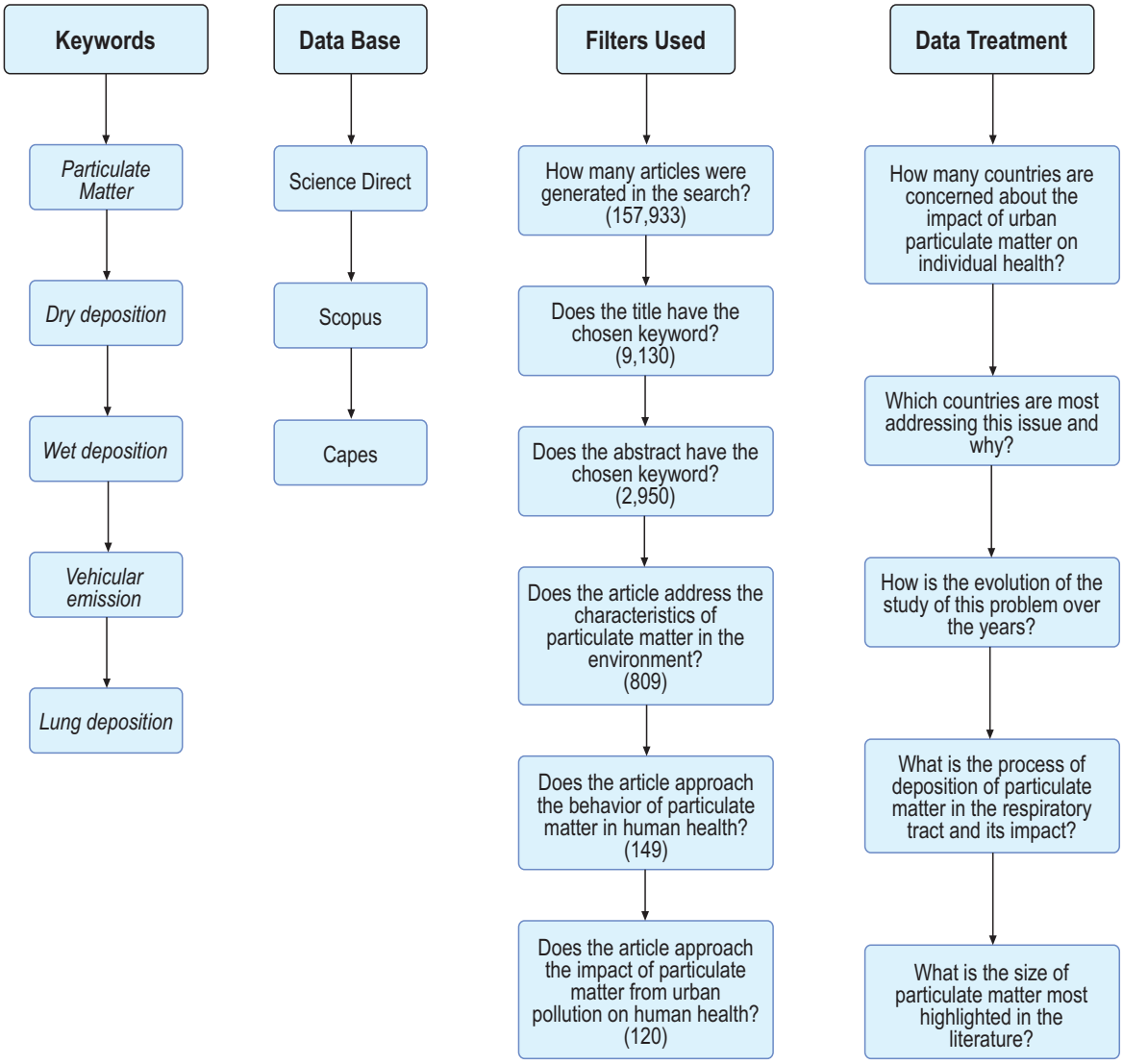

that the smaller the particle, the higher the ability to absorb organic and inorganic compounds, and the higher the ability to penetrate the respiratory tract [4]. The coarse particles (PM10), when inhaled, are lodged in the trachea (upper throat) due to the rubbing of the PM10 with the nasal hair, and then it will be harder to penetrate the expiratory system [4].

The fine particles (PM2.5) were highlighted in the literature as providers of high-risk diseases, and its capacity for higher emission is from vehicles exhaust (product of incomplete combustion of internal combustion engines) [10]. When inhaled (PM2.5) travels through the bronchioles and alveoli (where gas exchange occurs) and can penetrate the bloodstream causing significant health problems [4]. The impact of PM10 and PM2.5 is found in the literature as they are related to other particle sizes, such as PM1.0, which, like PM2.5, has a more exceptional ability to penetrate deeper into the human being [11]. It can aggravate asthma, bronchitis, and other respiratory problems, leading to cardiovascular symptoms [11].

Exposure to PM can promote the incidence of high-risk diseases such as respiratory problems, exacerbation of the chronic respiratory disease,

Graphic 1. Percentage list of articles that approach the theme published over the years.

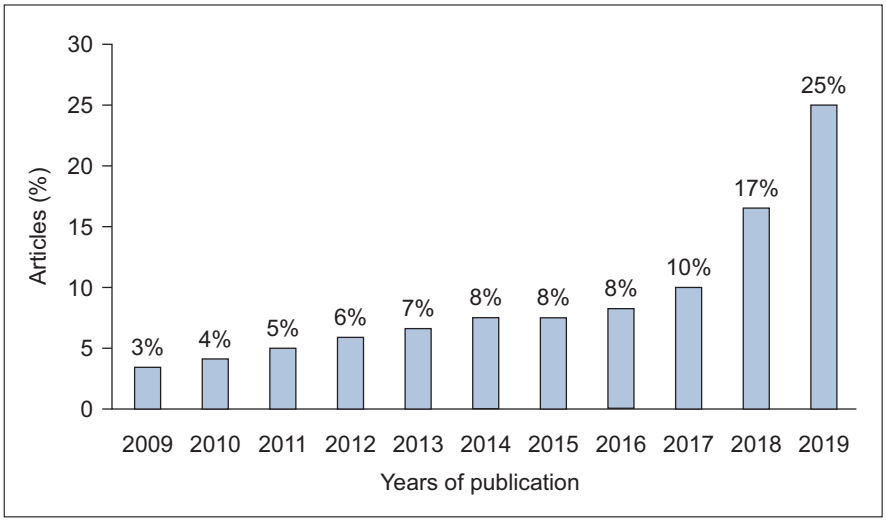

Graphic 2. List of countries that published the research theme the most.

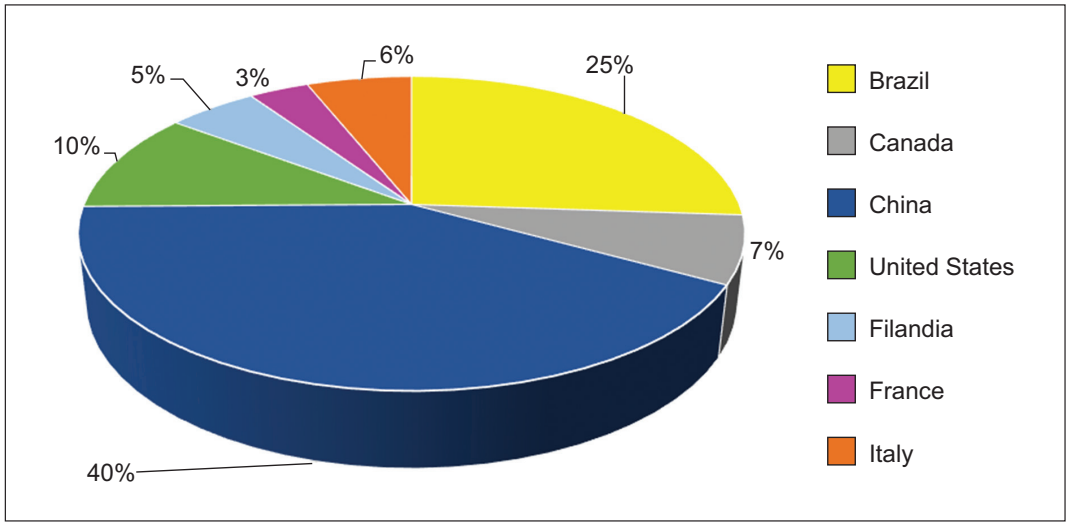

decreased lung function, premature mortality, as well as carcinogenic and mutagenic risks [4]. The PM emitted by the combustion of fuels is comprised of carbon, sulfur dioxide, unburned hydrocarbons, and some metals [12]. They have a strong relationship with the risk of lung cancer, as they cause damage to human DNA, by promoting breaks and alterations in the genetic chain (mutagenic effects) [12].

Therefore, because of their genotoxic (mutagenic) compounds, the emitted particles, especially smaller ones, have a high capacity to induce carcinogenic effects [4]. They can develop symptoms of lung cancer, in addition to other effects such as breathlessness, chest discomfort and pain, loud cough, and wheezing [4]. Children are more likely to be affected by the impact of PM in the respiratory tract as it can compromise lung development and function. Exposure to an excessive level of fine particles can mainly increase respiratory problems and carcinogenic effects [4].

Figure 2. Mortality and disease rates caused by ambient air pollution.

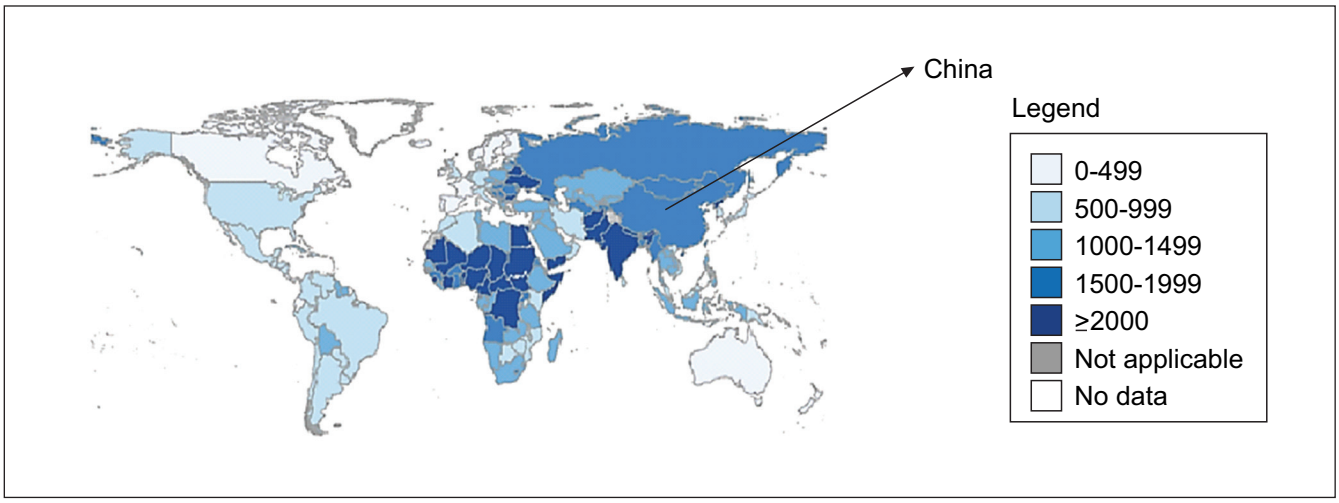

Source: WHO, 2018 [8].

Conclusions

This article focused on the impact that PM can have on human health, using a systematic review as a resource to obtain information in the literature to prove the problem mentioned. China has been identified as the country that publishes most articles on the subject, and this is justified by the fact that it has the highest degree of pollution from anthropogenic activities. The intense occurrence of this type of activity provides a high emission of fine PM, which, when deposited in the respiratory tract, can cause irreversible damage to human health.

References

1. ONU. 17 Objetivos para transformar nosso mundo. Available on: <https://nacoesunidas.org/pos2015/ods7/>. Access: Aug. 02, 2019.
2. Ali MU et al. A systematic review on global pollution status of particulate matter-associated potential toxic elements and health perspectives in urban environment. Environmental geochemistry and health. 2018:1-32.
3. WHO. Ambient (outdoor) air quality and health. Available on: <https://www.who.int/en/news-room/fact-sheets/detail/ambient-(outdoor)-air-quality-and-health/>. Access: Aug. 05, 2019.
4. Kim K-H, Kabir E, Kabir S. A review on the human health impact of airborne particulate matter. Environment International. 2015;74:136-143.
5. Hu Z et al. Concentrations and source apportionment of particulate matter in different functional areas of Shanghai, China. Atmospheric Pollution Research. 2014;5(1):138-144.
6. Dedelé A, Miskinyté A. Seasonal and site-specific variation in particulate matter pollution in Lithuania. Atmospheric Pollution Research. 2019;10(3):768-775.
7. Wang, S. et al. Size-fractionated particulate elements in an inland city of China: Deposition flux in human respiratory, health risks, source apportionment, and dry deposition. Environmental Pollution. 2019;247:515-523.
8. WHO. Mortality and burden of disease from ambient air pollution. Available on: <https://www.who.int/en/news-room/fact-sheets/detail/ambient-(outdoor)-air-quality-and-health/>. Access: Aug. 05, 2019.
9. Guarieiro LLN, Guarieiro ALN. Vehicle emissions: What will change with use of biofuel? In: Biofuels -Economy, Environment and Sustainability. [s.l.] InTech, 2013.
10. Wong YK et al. Estimating contributions of vehicular emissions to PM2. 5 in a roadside environment: A multiple approach study. Science of The Total Environment. 2019;672:776-788.
11. Karri RR et al. Modeling airborne indoor and outdoor particulate matter using genetic programming. Sustainable Cities and Society. 2018;43:395-405.
12. Guerrera E et al. Cytotoxicity and genotoxicity of size-fractionated particulate matter collected in underground workplaces. Air Quality, Atmosphere & Health. 2019;12(3):359-367, 2019.

An Innovative Concept of Traceable Device for Monitoring Temperature of Temperature-Sensitive Healthcare Products

Pedro Martins de Oliveira[1]*; Adriano Souza Leão[1]; Regina Maria Cunha Leite[1]; Alfredo Ruben Corniali[1]; Marcos Lage Cajazeira Ramos[1]; Valter Estevão Beal[1]
[1]SENAICIMATEC University Center; Salvador, Bahia, Brazil

This paper aims to present a concept of technology as a solution to monitor thermo-sensitive health products and contribute to preserving their integrity along the cold chain. This study is exploratory research with a case study involving a survey with health professionals and the use of tools for product development in order to find a solution to the problem of traceability and warnings about temperature deviations. From the information collected and the literature reviewed, it was possible to develop a concept of a product to meet the customer requirements. The results showed that thermo-sensitive health products lack traceability in the health network and that the concept presented contributes to solving this problem.

Keywords: Heat-Sensitive Products. Coldchain. IoT. Temperature Sensors.

Abbreviations: CCC (Cold Chain Central); WHO (World Health Organization); TSHP (Temperature-Sensitive Healthcare Products), GPM (Good Manufacturing Practices); QFD (Quality Function Deployment); BUHS (Brazilian Unified Health System).

Monitoring the thermal stability of Temperature-Sensitive Healthcare Products (TSHP), temperature control with the adoption of Good Manufacturing Practices (GPM) over all stages of the logistic chain, comprises an essential challenge to the sector. The "cold chain" - technology and process - integrates multiples logistic and packaging stages of the products. Therefore, it is fundamental to evaluate, in an integrative manner, the equipment used to monitor, control, preserve, store and transport, and to maintain the temperature at each stage throughout the entire chain.

Healthcare products, such as vaccines, insulin, eye drops, biopharmaceuticals, laboratory reagents, blood derivatives, and other products, are sensitive to temperature deviations. Most of the TSHP must have their temperature monitored, and be kept at adequate conditions of storage and transport to guarantee their integrity and efficiency according to the "Cold Chain Manual" of the National Immunization Program [1] and the "Cold Chain Manual" of the National Foundation of Health [2].

Two ranges of temperatures are primarely used and, therefore, at the Cold Chain Central (CCC), it must be stored and distributed with laboratory refrigerators (+2°C to +8°C) and freezers (-25°C to -15°C). Also, it is vital to keep a room for distribution, as well as a reception and inspection area.

It is crucial to guarantee the tracking of the TSHP across the entire cold chain in order to avoid damage caused by exposure to high temperatures [3] or freezing the products.

The World Health Organization (WHO) estimates that approximately 50% of the vaccines produced worldwide reach their destination with integrity compromised due to a break in the cold chain [4]. The temperature monitored in the Brazilian hospitals' sector is still conducted manually [5,6]. The commonly observed issues are: thermometers are often not calibrated; the measurement methods are not certified; the ice packs are not controlled, among several other problems. In many cases, domestic fridges and styrofoam boxes are used to

Received on 24 September 2019; revised 26 October 2019.
Address for correspondence: Dr. Pedro Martins de Oliveira. Centro Universitário SENAI CIMATEC. Avenida Orlando Gomes, N. 1845 - Piatã Zip Code: 41650-010; Salvador, Bahia, Brazil. E-mail: pedromartins175@gmail.com. This study was selected from the V International Symposium of Innovation and Technology - SIINTEC (October 2019). DOI: https://doi.org/10.34178/jbth.v2i4.93

J Bioeng. Biotech. Appl. Health 2019;2(4):141-146

maintain the temperature. The correct conservation and preservation of the TSHP must be a priority to all players involved, primarily because of thermal disturbances through the cold chain that may compromise product safety on its final use [1].

This article presents a concept to technology as a solution of monitoring the TSHP, which can contribute to preserving the integrity of TSHP along the cold chain. Exploratory research with a case study was conducted, comprising a survey with the cold chain professionals and the use of product development tools to find an innovative solution to the problem.

The Brazilian Cold Chain of TSHP

The stability of a healthcare product depends directly on the maintenance of the preset conditions over a certain period, preserving the physical integrity, power, purity, and efficiency [7]. One can state that once the TSHP is kept within the specified limits, at the end of the chain, the product will present the same characteristics as it had right after manufacturing, which means a guarantee of both therapeutic and diagnostic efficiency [8]. Figure 1 represents the logistic life cycle of the TSHP in the Brazilian scenario.

At the beginning of the cycle, the product is bundled at specific packages for each application, containing multiple protections for its physical integrity. It might include a primary package, as well as a secondary package (boxes with thermal insulation), not only for thermal protection but also for temperature preservation. Therefore, the TSHP can be delivered by the producer to the GMP under all certification criteria.

The first stop of the TSHP journey is a distribution center. During transportation, the carrier must protect the product against breakage, tampering, and theft, as well as ensure that temperature conditions would be maintained within the preset thresholds. The temperature maintenance has to consider the environmental conditions to which the product is exposed. Thus, energy provision is often needed.

After the reception of the product at the distribution center, the temperature is measured manually; and the product will be sent to the next destination with another transporter. The next step happens in drug storages inside hospitals, clinics, or vaccination centers. The products are received and stored in lab refrigerators and freezers to preserve the TSHP, where they manually measure temperature, which is controlled daily. These devices have precise temperature adjustment and several malfunction alarms. It is important to note that no cold chain manual has a prominent warning about household equipment, which is not recommended for TSHP storage, nor allowed to use the mini-bar fridge [1]. Even so, household equipment is widely used.

Due to the lack of control mechanisms, products are exposed due to power outage, shutdown, inadvertent door opening, and others that can undesirably change their temperature conditions. In those facilities, the products must remain in proper conditions as long as needed until their use is determined, e.g., in a patient's treatment or procedure.

During internal handling and transport, temperature control is also performed manually until the product is used, but no mechanism allows its traceability or data integration from end-to-end along the cold chain. Thus, there is no guarantee that the product has not lost the proper temperature condition by either raising or lowering the temperature outside its limits. These deviations may cause product loss.

Figure 1. Cold chain life cycle.

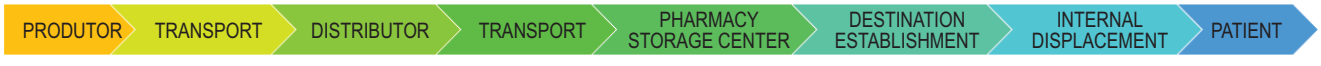

There are two key strategies to ensure integrity throughout the process: one is the "equipment validation" upon assessment and reliability. Other is the "processes qualification" that records, controls, and audits the procedures performed. Thus, traceability data can be obtained to monitor cold chain operations [1].

In Brazil, the lack of vehicles and highways in proper condition can affect logistics and, as a consequence, the quality of products transported, as it is a continental country and the most used mean of transportation is road type, reaching 59% [7]. The lack of adequate equipment for product storage and temperature control methods can also be as weak points.

Materials and Methods

The research strategy chosen was the case study due to the need to understand the situation of the health sector and propose a conceptual solution. The study was developed in two steps. Firstly, an understanding of the situation, secondly, the study of the solution (Figure 2).

The first stage consisted of identifying and understanding the problem. A survey with managers and other professionals with relevant functions in the public and private health network was conducted aiming to diagnose the transportation and storage situation of products in the TSHP network in Brazil. Questionnaires were sent to 50 professionals, and 18 replies were received. A literature review was also carried out in order to learn the available technologies, competitors, and patents. To understand the appropriate steps for the development of a product, we studied the life cycle of a TSHP. Thus, it was possible to identify customer needs.

In the second step, project requirements were translated from customer needs. A QFD Matrix was built to rank the project requirements, ordered by their importance to the customer. Then, a functional synthesis was made to identify the functions that the product should perform, which yielded a basis for the morphological Matrix. Then, the concepts were generated, and a winning concept was selected after a ranking analysis. This concept was indicated in this study as a solution.

Figure 2. Research design.

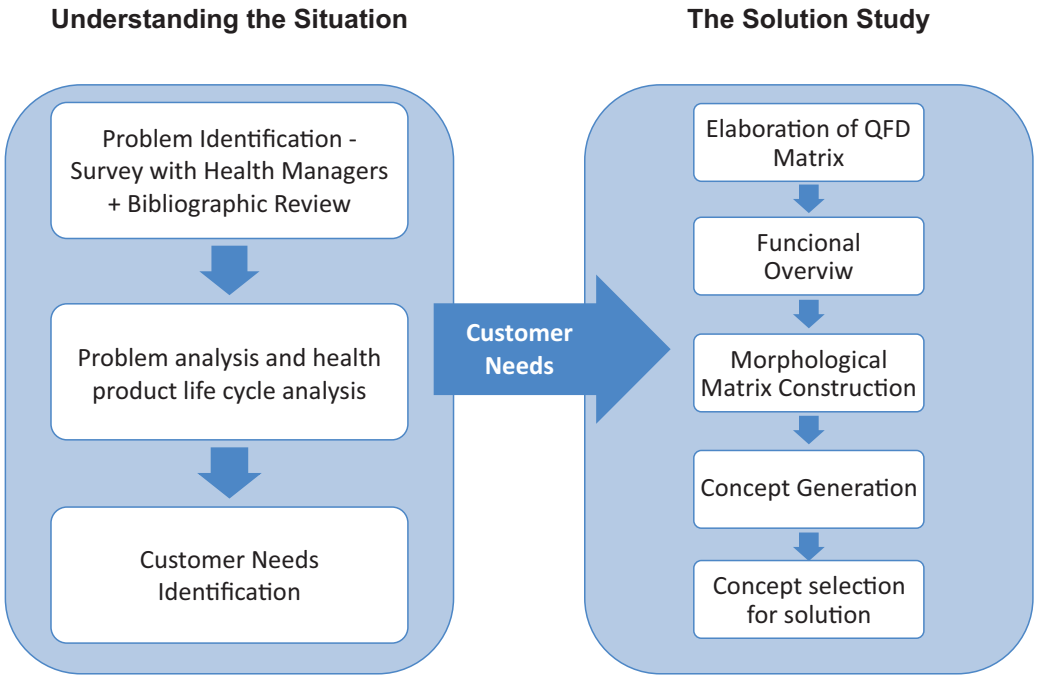

Diagnosis of the Situation in the Health Network

Key customers throughout the lifecycle were identified to gather information about their needs, whereas their assessments would be representative of the overall process. BUHS professionals, hospitals, clinical analysis laboratories, pharmacies, and carriers were consulted. The first questionnaire with 14 questions was prepared using the Google Forms tool, seeking to collect data as fully as possible, avoiding invasiveness as well as biasing of the questions.

Then, once the customer needs were identified, the respondents were asked to indicate aspects not mentioned before but deemed relevant. After that, they were asked to sign values to the needs according to their activity.

The Concept Generation Process

In total, 17 needs were identified. Then, a QFD Matrix was developed, also known as a 'Quality House', which is a method that transforms customer needs into project requirements [11]. These must be measurable in order to be transformed into useful product characteristics, so-called concepts), by the engineering perspective. Then, the requirements were listed and sorted by importance to the customer. The main requirements were: (1) reliability, (2) a low number of equipment failures per time of use, (3) minor errors in temperature measurement, (4) optimal amount of information provided, (5) low reject rate of TSHP and (6) low production cost.

The essential requirement is the reliability of the patient or healthcare professional. The following five needs show the importance of screening for healthcare professionals. End-to-end tracking of a product is a crucial procedure to ensure health care quality. Moreover, the low-cost of production appear to implement this type of innovation feasible.

Then, a functional synthesis was performed, which unfolded the function of tracking health products into five sub-functions: (1) receipt, (2) transportation, (3) storage, (4) local handling and transport, and (5) application / patient use.

A morphological matrix was constructed over a detailed study of each subfunction. A morphological matrix is a tool that systematically allows studying possible combinations between the components of a product [12]. It consists of a table in which the first vertical column contains the characteristics of the functions and subfunctions, and the horizontal lines contain the alternatives for each subfunction [12]. To aid the idea generation process for an ideal solution, the TRIZ Matrix was used, a method created by the Russian Genrich Altshuller in the mid-1940s, which uses 40 inventive principles to resolve technical contradictions [13].

From the analysis of the Morphological Matrix, six different concepts were obtained. Then, they were assessed seeking an ideal solution, aided by the Pass-Fail Evaluation method [12] in two rounds. In the first round, the six concepts were assessed and qualified. In the second round, the three concepts with the highest scores from the first round were used, resulting in a winning concept.

The Winning Concept

From the morphological matrix, the client's need could be understood and translated into different concepts that meet this demand. After assessing these concepts, it was possible to select a winning concept (Figure 3).

The proposed solution stands out for its innovative concept, where it tracks the TSHP to the end-user, and a system allows storing administrative information of the monitored product (Product, Lot No., Expiration Date, Invoice No.) as well as location, from the system reference antennae. It meets the demands obtained by the analysis of customer needs and has the potential for success against competitors and similar products found in the market.

Amongst the advantages that can be highlighted, one is the verification of product integrity through the dynamic reading of the data tracked and stored in the cloud/server logistics management system. The Ultra Narrow Band system, with low data transmission at low throughput, is responsible for

Figure 3. The selected concept and characteristics.

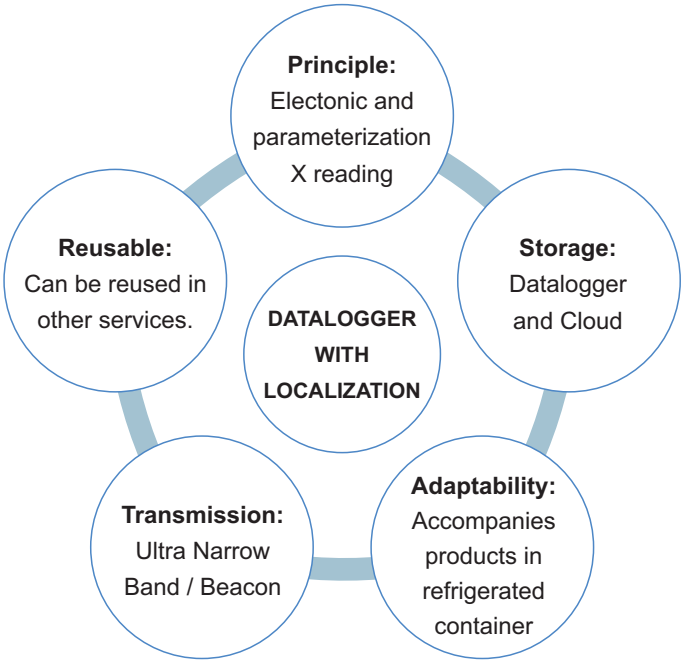

Features

- Electonic principle - Termistor;
- Parameterization x Reading;
- Accompanied in refigerated container;
- It has motion sensor, internal location (<10m bubble);
- Stores information in Datalogger and Cloud (real time remote access);
- Performs data transmission by Ultra Narrow Band / Beacon;
- It is reusable, has 130bpi e-ink, LED, BLE and Bidirectional Screen;
- It has 5 years battery, Bluetooth 5.0 with directional location with a range between 30 and 50 meters, carries all the information and updates the distance.

system communication, yet robust, and has a low interference rate.

Final Considerations

The medical industry manages high-cost and value-added products. Such products, if mismanaged, can result in severe financial and moral damage to institutions. The market analysis of products and services that depend on the cold chain allowed an understanding of the temperature control needs of TSHPs as well as working on the weaknesses that have become strengths of the concept presented.

Furthermore, the innovation industry is striding towards integrated data and information systems, where IoT appears as one of the main features of the new technological age. The winning concept can integrate the various actors along the cold chain (manufacturer, carrier, distributor, end consumer), and meeting the demands of traceability, both temperature and product location, a function that few competitors can achieve. This proposition could perform from end-to-end, integrating the logistics operation of these products and enabling the viewing of administrative data with no need to open the packaging, which represents a new application for the market.

References

1. Departamento de Vigilância Epidemiológica. Programa Nacional de Imunizações (PNI): 40 anos. Secretaria de Vigilância em Saúde. Ministério da Saúde. 2013.
2. Rocha CMV et al. Manual de rede de frio 3. Ed Brasília: Ministério da Saúde: Fundação Nacional de Saúde. 2001.
3. Ruiz-Garcia L, Lunadei L. Monitoring cold chain logistics by means of RFID. Sustainable Radio Frequency Identification Solutions. 2010;2:37-50.
4. Fiocruz. Os desafios da cadeia de frio na indústria farmacêutica. Bio-Manguinhos/FIOCRUZ. 2015. [Online] Available: https://www.bio.fiocruz.br/index.php/noticias/991-os-desafios-da-cadeia-de-frio-na-industria-farmaceutica. Accessed on Feb.12,2019.
5. Ávila A. Identificação por radiofrequência: tecnologia inteligente, hospital eficiente, qualidade e segurança para o paciente. Thesis. Instituto de Comunicação e Informação Científica e Tecnológica em Saúde, Fundação Oswaldo Cruz / Grupo Hospitalar Conceição. Rio Grande do Sul, 2012.
6. Alves ETA et al. Estudo de caso: sistema para monitoramento de temperatura e umidade em farmácias e almoxarifados. In: Congresso Brasileiro de Engenharia Biomédica. 2014:1208-1211.

7. Carvalho JS, Macedo SHM. Logística Farmacêutica Geral: Da Teoria à Prática. São Paulo. Contento. 2012.
8. Silva KER, Alves LDS, Soares MFR, Passos RCS, Faria AR, Rolimneto PJ. Modelos de avaliação da estabilidade de fármacos e medicamentos para a indústria farmacêutica. Rev. Ciênc. Farm. Básica Apl. 2009.
9. Kang S et al. Laboratory environment monitoring: Implementation experience and field study in a tertiary general hospital. Healthcare Informatics Research. 2018;24(4):371-375.
10. Roduit B et al. Continuous monitoring of shelf lives of materials by application of data loggers with implemented kinetic parameters. Molecules. 2019;24(12):2217.
11. Bolar AA, Tesfamariam S, Sadiq R. Framework for prioritizing infrastructure user expectations using Quality Function Deployment. International Journal of Sustainable Built Environment. 2017;6(1):16-29.
12. Amaral DC et al. Gestão de desenvolvimento de produtos. Editora Saraiva. 2017.
13. Altshuller G. 40 principles: TRIZ keys to innovation. Technical Innovation Center, Inc. 2002.

Instructions for Authors

The Authors must indicate in a cover letter the address, telephone number and e-mail of the corresponding author. The corresponding author will be asked to make a statement confirming that the content of the manuscript represents the views of the co-authors, that neither the corresponding author nor the co-authors have submitted duplicate or overlapping manuscripts elsewhere, and that the items indicated as personal communications in the text are supported by the referenced person. Also, the protocol letter with the number should be included in the submission article, as well as the name of sponsors (if applicable).

Manuscripts may be submitted within designated categories of communication, including:

- Original basic or clinical investigation (original articles on topics of broad interest in the field of bioengineering and biotechnology applied to health). We particularly welcome papers that discuss epidemiological aspects of international health, clinical reports, clinical trials and reports of laboratory investigations.
- Case presentation and discussion (case reports must be carefully documented and must be of importance because they illustrate or describe unusual features or have important practice implications).
- Brief reports of new methods or observations (short communications brief reports of unusual or preliminary findings).
- State-of-the-art presentations (reviews on protocols of importance to readers in diverse geographic areas. These should be comprehensive and fully referenced).
- Review articles (reviews on topics of importance with a new approach in the discussion). However, review articles only will be accepted after an invitation of the Editors.
- Letters to the editor or editorials concerning previous publications (correspondence relating to papers recently published in the Journal, or containing brief reports of unusual or preliminary findings).
- Editor's corner, containing ideas, hypotheses and comments (papers that advance a hypothesis or represent an opinion relating to a topic of current interest).
- Innovative medical products (description of new biotechnology and innovative products applied to health).
- Health innovation initiatives articles (innovative articles of technological production in Brazil and worldwide, national policies and directives related to technology applied to health in our country and abroad).

The authors should checklist comparing the text with the template of the Journal.

Supplements to the JBTH include articles under a unifying theme, such as those summarizing presentations of symposia or focusing on a specific subject. These will be added to the regular publication of the Journal as appropriate, and will be peer reviewed in the same manner as submitted manuscripts.

Statement of Editorial Policy

The editors of the Journal reserve the right to edit manuscripts for clarity, grammar and style. Authors will have an opportunity to review these changes prior to creation of galley proofs. Changes in content after galley proofs will be sent for reviewing and could be required charges to the author. The JBTH does not accept articles which duplicate or overlap publications elsewhere.

Peer-Review Process

All manuscripts are assigned to an Associate Editor by the Editor-in-Chief and Deputy Editor, and sent to outside experts for peer review. The Associate Editor, aided by the reviewers' comments, makes a recommendation to the Editor-in-Chief regarding the merits of the manuscript. The Editor-in-Chief makes a final decision to accept, reject, or request revision of the manuscript. A request for revision does not guarantee ultimate acceptance of the revised manuscript.

Manuscripts may also be sent out for statistical review ou *ad hoc* reviewers. The average time from submission to first decision is three weeks.

Revisions

Manuscripts that are sent back to authors for revision must be returned to the editorial office by 15 days after the date of the revision request. Unless the decision letter specifically indicates otherwise, it is important not to increase the text length of the manuscript in responding to the comments. The cover letter must include a point-by-point response to the reviewers and Editors comments, and should indicate any additional changes made. Any alteration in authorship, including a change in order of authors, must be agreed upon by all authors, and a statement signed by all authors must be submitted to the editorial office.

Style

Manuscripts may be submitted only in electronic form by www.jbth.com.br. Each manuscript will be assigned a registration number, and the author notified that the manuscript is complete and appropriate to begin the review process. The submission file is in OpenOffice, Microsoft Word, or RTF document file format for texts and JPG (300dpi) for figures.

Authors must indicate in a cover letter the address, telephone number, fax number, and e-mail of the corresponding author. The corresponding author will be asked to make a statement confirming that the content of the manuscript represents the views of the co-authors, that neither the corresponding author nor the co-authors have submitted duplicate or overlapping manuscripts elsewhere, and that the items indicated as personal communications in the text are supported by the referenced person.

Manuscripts are to be typed as indicated in Guide for Authors, as well as text, tables, references, legends. All pages are to be numbered with the order of presentation as follows: title page, abstract, text, acknowledgements, references, tables, figure legends and figures. A running title of not more than 40 characters should be at the top of each page. References should be listed consecutively in the text and recorded as follows in the reference list, and must follow the format of the National Library of Medicine as in Index Medicus and “”Uniform Requirements for Manuscripts Submitted to Biomedical Journals” or in “Vancouver Citation Style”. Titles of journals not listed in Index Medicus should be spelled out in full.

Manuscript style will follow accepted standards. Please refer to the JBTH for guidance. The final style will be determined by the Editor-in-Chief as reviewed and accepted by the manuscript’s corresponding author.

Approval of the Ethics Committee

The JBTH will only accept articles that are approved by the ethics committees of the respective institutions (protocol number and/or approval certification should be sent after the references). The protocol number should be included in the end of the Introduction section of the article.

Publication Ethics

Authors should observe high standards with respect to publication ethics as set out by the International Committee of Medical Journal Editors (ICMJE). Falsification or fabrication of data, plagiarism, including duplicate publication of the authors’ own work without proper citation, and misappropriation of the work are all unacceptable practices. Any cases of ethical misconduct are treated very seriously and will be dealt with in accordance with the JBTH guidelines.

Conflicts of Interest

At the point of submission, each author should reveal any financial interests or connections, direct or indirect, or other situations that might raise the question of bias in the work reported or the conclusions, implications, or opinions stated - including pertinent commercial or other sources of funding for the individual author(s) or for the associated department(s) or organizations(s), and personal relationships. There is a potential conflict of interest when anyone involved in the publication process has a financial or other beneficial interest in

the products or concepts mentioned in a submitted manuscript or in competing products that might bias his or her judgment.

Material Disclaimer

The opinions expressed in JBTH are those of the authors and contributors, and do not necessarily reflect those of the ITS/SENAI CIMATEC, the editors, the editorial board, or the organization with which the authors are affiliated.

Privacy Statement

The names and email addresses entered in this Journal site will be used exclusively for the stated purposes of this journal and will not be made available for any other purpose or to any other party.

Brief Policies of Style

Manuscript	Original	Review	Birief Comunication	Case Report	Editorial ; Letter to the Editor; Editor' s Corner	Innovative Medical Products	State-of-the-Art	Health Innovation Initiatives
Font Type	Times or Arial	Times or Arial	Times or Arial	Times or Arial	Times or Arial	Times or Arial	Times or Arial	Times or Arial
Number of Words – Title	120	90	95	85	70	60	120	90
Font Size/Space-Title	12; double space	12; double space	12; double space	12; double space	12; double space	12; double space	12; double space	12; double space
Font Size/Space-Abstracts/Key Words and Abbreviations	10; single space	10; single space	10; single space	10; single space	-	-	10; single space	10; single space
Number of Words – Abstracts/Key Words	300/5	300/5	200/5	250/5	-	-	300/5	300/5
Font Size/Space-Text	12; Double space	12; Double space	12; Double space	12; Double space	12; Double space	12; Double space	12; Double space	12; Double space
Number of Words – Text	5,000 including spaces	5,500 including spaces	2,500 including spaces	1,000 including spaces	1,000 including spaces	550 including spaces	5,000 including spaces	5,500 including spaces
Number of Figures	8 (title font size 12, double space)	3 (title font size 12, double space)	2 (title font size 12, double space)	2 (title font size 12, double space)	-	2 (title font size 12, double space)	8 (title font size 12, double space)	8 (title font size 12, double space)
Number of Tables/Graphic	7 title font size 12, double space	2 title font size 12, double space	2(title font size 12, double space)	1(title font size 12, double space)	-	-	7 title font size 12, double space	4 title font size 12, double space
Number of Authors and Co-authors*	15	10	5	10	3	3	15	10
References	20 (font size 10,single space	30(font size 10,single space	15 (font size 10,single space)	10 (font size 10,single space)	10 (font size 10,single space	5(font size 10,single space	20 (font size 10,single space	20

*First and last name with a sequencing overwritten number. Corresponding author(s) should be identified with an asterisk; Type 10, Times or Arial, single space. Running title of not more than 40 characters should be at the top of each page. References should be listed consecutively in the text. References must be cited on (not above) the line of text and in brackets instead of parentheses, e.g., [7,8]. References must be numbered in the order in which they appear in the text. References not cited in the text cannot appear in the reference section. References only or first cited in a table or figures are numbered according to where the table or figure is cited in the text. For instance, if a table is placed after reference 8, a new reference cited in table 1 would be reference 9.1 would be reference 9.

Checklist for Submitted Manuscripts

❑1. Please provide a cover letter with your submission specifying the corresponding author as well as an address, telephone number and e-mail.

❑2. Submit your paper using our website www.jbth.com.br. Use Word Perfect/Word for Windows, each with a complete set of original illustrations.

❑3. The entire manuscript (including tables and references) must be typed according to the guidelines instructions.

❑4. The order of appearance of material in all manuscripts should be as follows: title page, abstract, text, acknowledgements, references, tables, figures/graphics/diagrams with the respective legends.

❑5. The title page must include a title of not more than three printed lines (please check the guidelines of each specific manuscript), authors (no titles or degrees), institutional affiliations, a running headline of not more than 40 letters with spaces.

❑6. Acknowledgements of persons who assisted the authors should be included on the page preceding the references.

❑7. References must begin on a separate page.

❑8. References must be cited on (not above) the line of text and in brackets instead of parentheses, e.g., [7,8].

❑9. References must be numbered in the order in which they appear in the text. References not cited in the text cannot appear in the reference section. References only or first cited in a table or figures are numbered according to where the table or figure is cited in the text. For instance, if a table is placed after reference 8, a new reference cited in table 1 would be reference 9.

❑10. Reference citations must follow the format established by the "Uniform Requirements for Manuscripts Submitted to Biomedical Journals" or in "Vancouver Citation Style".

❑11. If you reference your own unpublished work (i.e., an "in press" article) in the manuscript that you are submitting, you must attach a file of the "in press" article and an acceptance letter from the journal.

❑12. If you cite unpublished data that are not your own, you must provide a letter of permission from the author of that publication.

❑13. Please provide each figure in high quality (minimum 300 dpi: JPG or TIF). Figure must be on a separate file.

❑14. If the study received a financial support, the name of the sponsors must be included in the cover letter and in the text, after the author's affiliations.

❑15. Provide the number of the Ethics Committees (please check the guidelines for authors).